16

Analogue CMOS Cochlea Systems: A Historic Retrospective

Andreas Katsiamis and Emmanuel Drakakis
Imperial College London
United Kingdom

1. Introduction

For more than twenty-five years, the bionics community (and particularly the VLSI engineering community) has been performing extensive research to understand, model and design in silicon the biological auditory system and specifically the inner ear or cochlea. The aim of this on-going effort is not only towards building the ultimate artificial speech processor or implant, but also to develop systems that can contribute towards a deeper understanding of the underlying engineering strategies that nature chose to espouse. For these reasons, certain parts of the VLSI engineering community believe that trying to mimic certain biological operations will, in principle, yield systems that are somewhat closer to nature's power-efficient computational ability.

However, engineers must identify what they should and what they should not directly replicate in an artificial system inspired from biology. As for example, it does not make sense to create commercial aircraft wings to flap like those of birds (even though unmanned flapping-wing aircrafts are currently being developed – check NASA's flapping solar aircraft) it is equally meaningful to argue that not all operations of the cochlea can or should be replicated in silicon in an exact manner. Abstractive operational or architectural simplifications dictated by logic and the available technology have been crucial for the successful implementation of useful hearing-type machines. Moreover, the biological cochlea is a three-dimensional electro-hydro-mechanical system, whereas most electronic systems are one-dimensional systems. Based on these thoughts, it would be wise to try and clarify three terms that are commonly used in the (bio-) engineering literature. Namely, these are:

- Neuromorphic: the system level architecture is designed in such a way in order to replicate 'exact' basic anatomical identified operations which embody several key features encountered in the biological system. The term 'neuromorphic' was introduced by ***Carver Mead*** in (Mead, 1989;Mead, 1990) .
- Bio-inspired: the design and/or operation are based on (inspired from) the engineering principles underlying its biological counterpart.
- Biomimetic: the behaviour/operation/response resembles the one directly observed from the biological system, applying completely, partially or not at all the engineering principles encountered in the biological system.

It should be therefore evident that a neuromorphic design is also bio-inspired and biomimetic, whereas a biomimetic (or bio-inspired) design is not necessarily neuromorphic. We shall provide tangible examples on this fact as the chapter unfolds.

Since the late seventies, there we numerous attempts from several research laboratories to capture the main attributes of the biological cochlea in a way that are conveniently (i.e. computationally efficiently) replicated in silicon. This chapter attempts to present a rather detailed historical retrospective of nearly twenty-seven years of analogue VLSI cochlea development. The chapter is organized in ascending chronological in order to unravel the chain of events in order to appreciate how the research direction changed through time. If the reader wishes to skip all the details, s/he can refer to Table 1 and Fig. 32 at the end which summarizes the performances of the most important efforts.

2. The early years: 1982 - 1992

1982: The first to sow the seeds for the coming generations of VLSI engineers was ***Richard F. Lyon*** who in 1982, while in Fairchild Artificial Intelligence Research Laboratory, proposed a VLSI-compatible computational model of filtering, detection and compression in the cochlea (Lyon, 1982), even though it seems that he had conceived the idea earlier – check one of his unpublished efforts circa 1978 (Lyon, 1978). His work made a clear link to the early Wegel and Lane (Wegel and Lane, 1924) and Fletcher (Fletcher, 1930) model of micromechanics (the one-dimensional passive transmission line model) and to the more recent model of non-linear differential equations by Kim and his associates (Kim et al., 1973). In this pioneering work, the proposed model (which was later given the name: 'The Lyon's Cochlear Model' by Malcolm Slaney (Slaney, 1988)) cleanly separated the effects of mechanical filtering in the BM into time-invariant linear filtering based on a simple cascade/parallel filterbank network of second-order sections (or biquad filters). Lyon apart from BM filtering also discussed that detection and compression should be incorporated in the final model by means of half-wave rectification and a coupled nonlinear AGC network. Lyon's cochlea model can be described briefly as follows:

Wave propagation in distributed non-uniform media like the BM can – in principle – be modelled by a cascade of filters. Such a cascade will give rise to overall transfer functions with sharp roll-off slopes corresponding to higher-order structures. This kind of BM modelling relies upon the approximation that for a short BM section Δx, the parameters change only slightly and thus it behaves just as a short section would in a uniform medium. *In other words, the non-uniform medium can be discretised with each portion assumed to be locally uniform*. Each of these uniform portions can be modelled by a filtering stage which alters the magnitude and phase of excitation. The parameters of each successive filter (corresponding to a different Δx segment) will scale accordingly so that the collective response of the whole cascaded structure approximates the behaviour of the non-uniform medium.

In this first attempt, each BM segment was approximated as a lowpass notch (LPN) transfer function with the resonance frequencies, that determine the notch locations, changing approximately exponentially (modelling how the properties of the BM change lengthwise) from 20kHz at the input end (base) to 50Hz at the output end (apex). The cascaded LPN filters conspired to create a collection of lowpass filters (LPF) with very steep high-frequency roll-off slopes. A resonator transfer function, a simple bandpass filter (BPF) was added at the output of each LPN output (tap) to convert BM displacement to BM velocity. The overall effect was a BM cochlea 'tuning curve' which qualitatively had an asymmetric BP shape much like the one Rhode observed in the early 70s.

This cascade/parallel filterbank architecture constitutes part of a single-input, multi-output system with a very useful property: the sum of the orders of the transfer functions from the

input to each output (tap) greatly exceeds the sum of the orders of the component sections, thus achieving an economy of computation by using the same low-order section in many high-order transfer functions. The filter-cascade also enforces uni-directionality of energy (not allowing the introduction of reflections which could lead to instability) and achieves a high-gain pseudo-resonance by coupling the individual low-gain stages forming the cascade. A block diagram of the cascade/parallel architecture is shown in Fig. 1, whereas Fig. 2 shows the frequency responses of its constituent transfer functions.

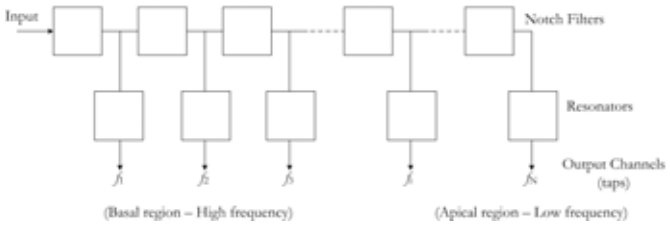

Fig. 1. Block diagram of the cascade/parallel filterbank for modelling travelling wave propagation in the BM; adapted from Lyon (Lyon, 1982).

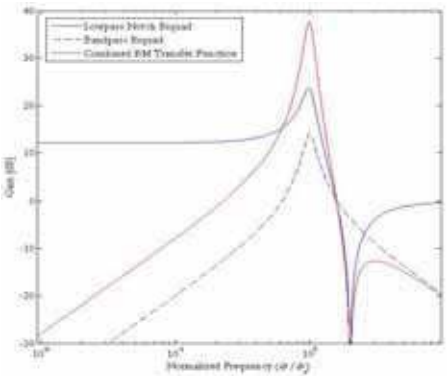

Fig. 2. Indicative transfer functions of the LPN, resonator and their combined response resembling the one obtained from a particular output tap.

1988: Even though Lyon's 1982 paper provided a very useful insight on how BM wave propagation could be modelled using basic second-order building blocks, his proposed AGC scheme, while carefully thought, seemed quite underdeveloped regarding a real-time neuromorphic circuit implementation. *In his 1982 effort, all the filters forming the BM where linear time-invariant transfer functions with the AGC providing a straight gain variation at the output of each tap. Moreover the gain control responded to the system's measured output level and not the input level*. This AGC scheme was quite different from what is really happening in reality since the peak gain of the cochlea filters changes dynamically with input level and not by providing separate amplification after the filtering stage. It took almost six years for the big contribution to arise. In 1988 the very first CMOS cochlea was presented. The paper 'An Analog Electronic Cochlea', co-authored with ***Carver Mead***, won an IEEE best paper award and cemented the current views on how the basic functions of BM together with its vestibular apparatus can be modelled in silicon (Lyon and Mead, 1988a;Lyon and Mead,

1988b). Even though the cornerstone was placed in 1982, it was this work that presented Lyon's modelling ideas in a more complete and unified way.
In this particular design effort, each BM segment was modelled as a LP biquad (although the initial 1982 model used LPN biquads) with no resonator stages connected to each of the outputs. The LP biquad (generally easier to design in silicon than a transfer function containing zeros) was a natural choice for modelling BM filtering, because it is passive and linear for low frequencies and provides gain near the peak or centre frequency (CF) while attenuating high frequencies.
Although, the frequency selective properties of the BM were modelled as a collection of linear, time-invariant transfer functions, sufficient evidence shows that the cochlea is highly nonlinear. The filtering architecture presented in this paper did not differ conceptually from the one presented in 1982. However, a scheme for a possible *neuromorphic* circuit implementation of the coupled AGC network was presented here for the first time. Lyon understood that for the purposes of speech analysis, the nonlinear behaviour of the cochlea could be adequately accounted for by lumping it in the compression mechanism of the AGC. Contrary to what he had shown in 1982, here he proposed that *by adaptively varying the quality factors (Q) of the individual filter stages in response to the input intensity level, overall large gain variations could be achieved for the combined response.* Since the whole cascade structure is essentially a very high-order system, the *Q* of the individual filters only need to vary by little in order to achieve large gain variations. In other words, the effect of the OHC-based AGC was modelled as a local fast-acting adaptation of the *Q* for each BM stage: as a signal of particular frequency and amplitude travels along the cascade, each filter section will adjust its *Q* value so that the collective pseudo-resonant transfer function tunes in accordance to the particular input excitation. In this way a large detected signal at one place could reduce the gain at nearby places and give rise to outstanding scale-invariant and matching properties along the cascade.
Lyon suggested at the time, that the actual local feedback for each stage would involve a half-wave rectifier connected directly after the stage's output tap (modelling the operation of the IHC, since IHC fire when they are bend in one direction and cease firing when they are bend in the other), a strength detector to extract the intensity of the input signal and some kind of a *Q*-decision circuit that will map that intensity level to an appropriate biasing value for setting the *Q* of the particular filter stage. From all the above, it should be easy to see that Lyon's model is neuromorphic since the BM structure and its associate transducers are directly mapped onto circuit blocks that emulate their behaviour and operation.
The paper, apart from the thorough discussion on biological cochlea operation and mathematical modelling of wave propagation in non-uniform media, also discussed practical details on the circuit implementation of the biquad section. The LPF was designed in voltage-mode based on simple transconductance amplifiers (OTA) and capacitors (i.e. g_m-C) with all MOS devices operating in their weak inversion (WI) regime (see Fig. 3). Since in a WI MOS device a linear change in voltage corresponds to an exponential change in current, the exponential tapering of the cut-off frequencies was easily achieved by using a linear voltage gradient (through a resistive line) on the transistor gates. Finally, measured results from a 480-stage fabricated chip were provided showing LP constant-*Q* (i.e. the individual *Q* values were manually set off-chip) AC responses (see Fig. 4); no detailed discussion or results from an AGC or from an overall adaptively regulated system were provided. Even though Lyon proposed the architecture behind the aforementioned AGC scheme, he did not implement it, probably because of certain stability problems they were facing at the time.

Detailed results on power consumption, linearity, noise, dynamic range (DR) etc., were also not given.

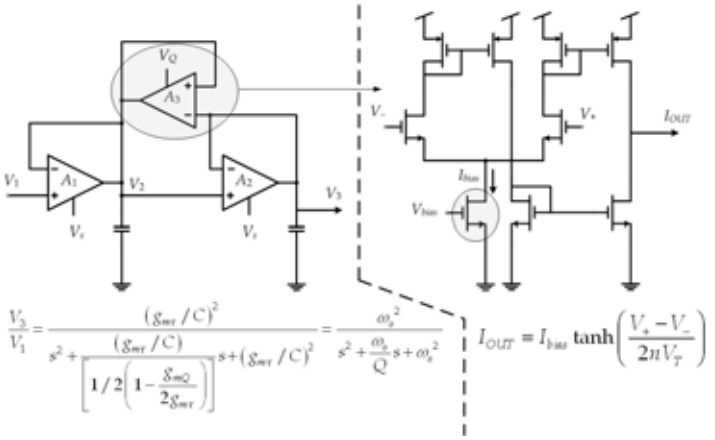

Fig. 3. The lowpass biquad circuit. The ω_o and Q control inputs set the OTA bias currents for controlling the pole frequency and quality factor (and hence the peak gain) of the filter response. Amplifiers A_1 and A_2 have the same transconductance gm (left). The basic CMOS OTA circuit used for realizing amplifiers A_1, A_2 and A_3 (right). The implemented relations are shown beneath each circuit. Parameters V_T and n denote the thermal voltage and subthreshold slope parameter, respectively; adapted from Lyon (Lyon and Mead, 1988a).

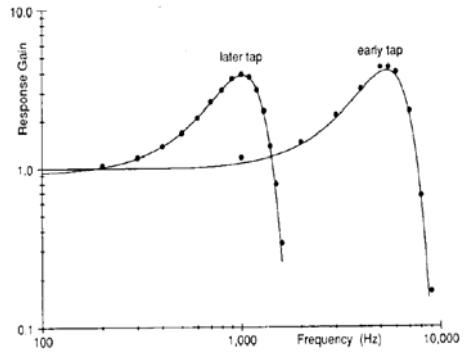

Fig. 4. Measured log-log frequency responses to two output taps (i.e. at particular BM locations) placed 120 stages apart. The stages Q were manually adjusted to 0.79; from Lyon (Lyon and Mead, 1988a).

1989&1990: One year later in Japan, ***Tatsuya Hirahara*** published a conference paper on a computational nonlinear model with adaptive Q circuits (Hirahara and Komakine, 1989). Even though the word 'circuits' was used both in the title and numerous times in the text, no circuits or indications of how to build them were presented. The paper reported on system level ideas by showing the equations and basic transfer functions of the blocks comprising a 61-stage cascade. Hirahara's main idea was based on Lyon's cascade/parallel 1982 model, but included a model on the actual decision block that specified which input

amplitude corresponded to which Q for each filter stage of the cascade. In other words, it specified the law with which the filter stages adapted their gains at the presence of an input signal, essentially modelling the effect of OHC (see Fig. 5). To this author knowledge, this effort was one of the very first to elaborate on the Q-control law.

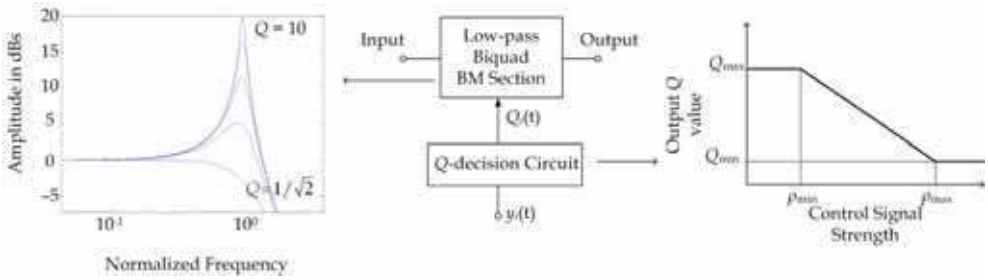

Fig. 5. Block diagram of the adaptive Q function (middle), frequency response of a biquad LPF left) and input-output relationship of the Q decision block which calculates the LP Q values according to (input or output) signal strength. For a large control signal (ρ_{max}), the Q value is minimum and the LP response becomes passive providing no gain at the peak frequency. On the other extreme (ρ_{min}), the Q value is maximum and the LP response becomes selective providing maximum gain for frequencies near the peak frequency. The relationship between the two extremes is linear; adapted from Hirahara (Hirahara and Komakine, 1989).

Around the same time ***John Lazzaro*** from Carver Mead's group at Caltech, continued Lyon's work and proposed silicon integrated circuits that modelled sensory transduction in the cochlea (Lazzaro and Mead, 1989a). His cochlea chip (based on filter-cascades and using the same g_m-C filters as the ones Lyon had used earlier) was neuromorphic because once again it captured the structure as well as the function of the cochlea with all the proposed subcircuits having anatomical correlates. In this effort, the very first CMOS IHC circuit model was presented consisting of a hysteretic differentiator that performed both logarithmic compression (proposed by Mead in (Mead, 1989)) and half-wave rectification. The function of the hysteretic differentiator was to convert BM displacement to BM velocity while enhancing the zero-crossings of the input waveform, thereby emphasizing its phase information. The input of the IHC was attached at each BM section tap, whereas the output was connected to a spiral-ganglion-neuron (SGN) circuit (a slightly modified version of the neuron circuit also proposed by Mead in (Mead, 1989)) that converted the (uni-directional) half-wave rectified current waveform into fixed-width, fixed-height voltage pulses (see Fig. 6). The average pulse rate and the temporal placement of each pulse reflected the average value and shape of the IHC half-wave rectified waveform, respectively. The pulsed output was then delayed by a time matched to the resonant frequency of its associated cochlea tap and consequently correlated (through a simple CMOS AND gate) with the initial pulsed waveform to create the final output. The resulting *matched filter* operation resembled in frequency a sharply tuned BP response with the maximum spike rate corresponding to the CF of the particular tap.

Lazzaro inserted pure sinusoidal tones to his cochlea chip and measured the rate (in spikes per second) from the output of each silicon auditory nerve. His results were useful additions to Lyon's initial BM frequency-response measurements because he managed to faithfully

reproduce a variety of physiological auditory nerve responses. His integrated circuit model captured many essential features of data representation in the auditory nerve, in real-time and over a 60dB of input DR. Indicative results are shown in Fig. 7. Nevertheless, as with Lyon's effort, Lazzaro still did not implement the OHC circuits to obtain responses from an adaptively regulated system.

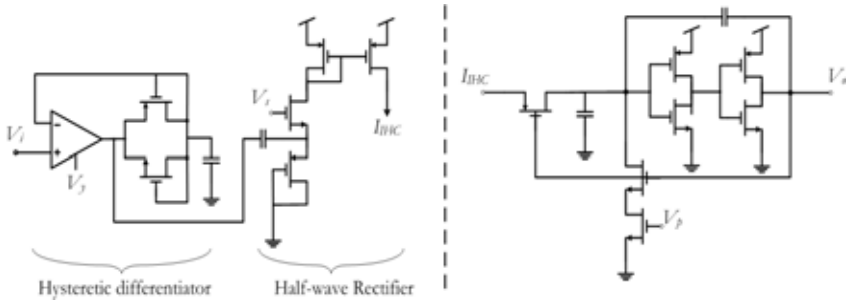

Fig. 6. The IHC (left) and SGN circuit models (right). The input V_i from the BM filtering stage is a time-varying voltage waveform. The hysteretic differentiator, biased with a voltage V_y performs time-differentiation and logarithmic compression. The output from the hysteretic differentiator goes to a half-wave current rectifier circuit. The uni-directional output current from the IHC circuit goes to the SGN circuit which converts it into fixed-width, fixed-height voltage pulses at the output V_o. The bias voltage V_p sets the pulse width with V_o pulsating between the supply and ground; adapted from Lazzaro (Lazzaro and Mead, 1989a).

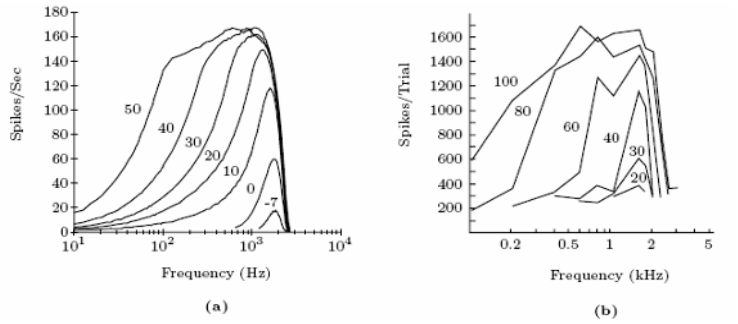

Fig. 7. (a) Measured chip plots showing the mean spike rate of a silicon auditory fibre as a function of pure tone frequency. (b) Physiological plots showing the number of neural discharges of an auditory fibre in the squirrel monkey in response to a 10sec pure tone. Tone amplitudes in dB are indicated on each plot; from Lazzaro (Lazzaro and Mead, 1989a).

Lazzaro's work did not stop there. He was also the first to apply his and Lyon's circuit modelling ideas for sound source localization (based on the passive localization system of the barn owl) (Lazzaro and Mead, 1990;Lazzaro, 1991) and for pitch perception (Lazzaro and Mead, 1989b). With the aid of Fig. 8, the operation of Lazzaro's localization system can be briefly described as follows:

Lazzaro integrated two cochlea cascades on the same chip which represented the left and right ears of the barn owl. The chip received its inputs from two separate signal generators

and the two 62-stage g_m-C cascades performed frequency decomposition causing a maximum excitation at a tap corresponding to the frequency of the input waveforms. The previously presented IHC and SGN circuitry consequently rectified and converted the output signals at each tap into pulses. Each pulse from the SGN circuit propagated down a silicon axon circuit; the direction of propagation being from left-to-right from the SGN of the left cochlea and from right-to-left from the SGN of the right cochlea. Thus, when a sound appeared at both chip inputs, action potentials counter-propagated across the chip. Circuit-wise, the axon was nothing more than a discrete delay line with the input being a fixed-width, fixed-height pulse which travelled along its length, section by section, at a controllable velocity. At any point in time, only one section of the axon was firing. Correlator circuits laid in between each pair of antiparallel axons and at every discrete section that connected directly to both axons. The simultaneous appearance of pulses at both inputs of the correlator initiated a maximum output response. If only one input was present, the correlator generated no output. In this way, interaural time differences could map into a neural place code. The final section of the chip was a circuit that performed a winner-take-all-function (a modified version of the circuit was used by ***Misha Mahowald*** and ***Tobi Delbrück*** in (Mahowald and Delbriick, 1989)), producing a new map of interaural time differences in which only one neuron had significant energy. The chip then multiplexed this final map on a single wire for display on an oscilloscope.

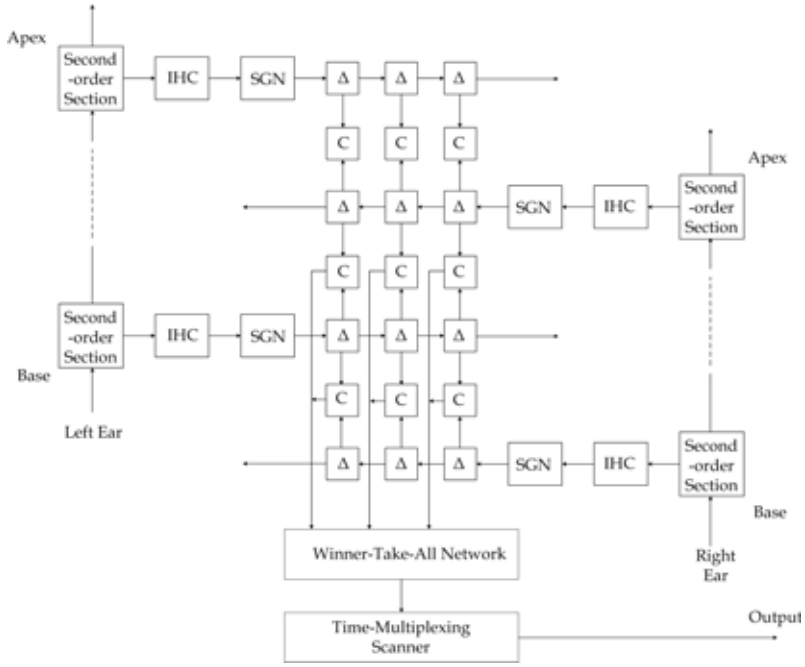

Fig. 8. Floorplan of the silicon model for sound localization of the owl. The square blocks marked with a 'Δ' represent the discrete delay elements forming the silicon axons, whereas the square blocks marked 'C' in between every antiparallel axon are the correlators or coincidence detectors which take two inputs from the upper and lower axons; adapted from Lazzaro (Lazzaro and Mead, 1990).

Lazzaro's contributions to the neuromorphic community were important because he managed to steer research towards a more application-specific direction. In the following years, quite a few researchers did significant work on the (re-)design and optimization of sound localization systems (using either neuromorphic or bio-inspired approaches) in an attempt to create artificial systems that could not only hear but also detect azimuthally or horizontally sound source locations. Applications were localization plays an important role include sound-guided robots and automatic camera orientation in teleconference systems.

1991: Two years later, an interesting paper was published by Lyon which addressed for the first time the key problems they were facing at Caltech with the first generations of cochlea chips (Lyon, 1991). *Lyon understood that the inherent exponential behaviour of MOS transistors in WI led – in general – to nonlinear filter circuits in which the small-signal and large-signal behaviours could be quite different.* He proposed that in order to overcome problems like poor DR, excessive noise (accumulating naturally in a long cascade) and instability, they would need to come up with the design of *inherently compressive* filter stages. Quoting Lyon: 'Tests on early second-order filter stages, including a low-noise version based on the MOSIS low-noise analogue BiCMOS process, revealed a problematic nonlinear effect related to the saturation of the *tanh* nonlinearity of the transconductance amplifiers. The filter stages ended up with more gain for large signals than for small signals (i.e. they were "expansive"), and the result was that a given periodic input could lead to a pair of distinct periodic attractors. In a cascade of such filter stages, when the input became large enough to kick any stage into its large-signal mode, the final result was a chaotic output waveform resembling fractal mountains'. That was quite an interesting observation, firstly because identifying this kind of misbehaviour was non-trivial at a time where simulation tools (let alone accurate WI MOS transistors models) were not as developed as they are now, and secondly because the first paper on filters which perform signal compression to increase their DR and lower their power consumption (the so called *companding* signal processors) was published around that same year (Seevinck, 1990;Tsividis et al., 1990). A systematic formulation for the design of companding filters followed almost two years later (Frey, 1993).

In this paper, Lyon explored two different biquadratic architectures (based on cascades of two- and three-OTA topologies, called DIFF2 and DIFF3 respectively in (Lyon, 1991)) and incorporated source degeneration and capacitive division to widen the linear range of the OTA comprising the filters. However, contrary to the implementation of Fig. 3, these designs had their Q and pole-frequency voltages interdependent leading to generally more difficult tuning schemes. Nevertheless, with these improvements, he managed to get a 40dB pseudo-resonance gain in the cochlea response, rather than the 12dB previously shown in Fig. 4 with a useable DR of about 40dB.

1992: After Lazzaro, the lead in the Caltech group was passed on to ***Lloyd Watts*** who was responsible for creating the first advancement in cochlea chip design since Lyon's original chip. Watts's overall design was based on a model of a passive (i.e. without an AGC network) 2-D cochlea (the first of its kind) (Watts, 1992). That model differs considerably from Lyon's 1-D filter-cascade, because it tries to replicate BM filtering together with the cochlea fluid. The fluid was modelled using a 2-D resistive network while the BM was modelled using g_m-C circuits which could mimic the BM impedance. Although the resulting system had ten times larger area than its 1-D equivalent, it had the advantages of exhibiting more realistic responses, being bi-directional (essentially modelling fluid reflections), fault-tolerant and having a continuum limit. A conceptual diagram of his proposed 2-D cochlea

model is shown in Fig. 9. Moreover, Watts was actually the first to propose a model for 'closing the loop' with OHC circuits, but his investigation ended prematurely. Quoting Watts: 'At the present time, the correct behaviour of the OHC circuit has not been verified at the system level, so we must leave the project as it is. Since there is still confusion in the auditory community about the form and sign of the mechanical feedback from the motile OHC…'.

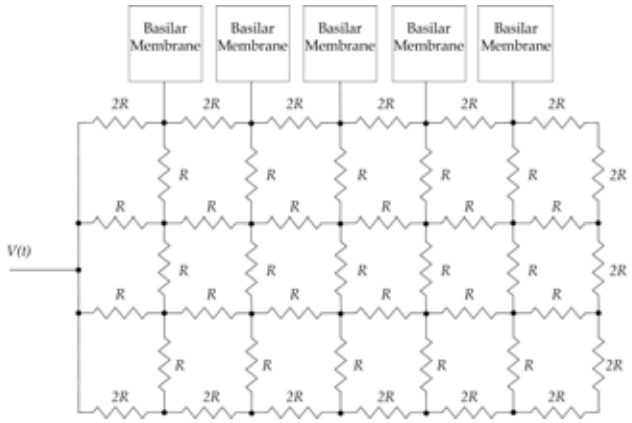

Fig. 9. The 2-D cochlea model. The cochlea fluid was modelled as a 2-D resistive network; adapted from Watts (Watts, 1992).

Apart from his 2-D contribution, Watts also thoroughly explored Lyon's 1-D cochlea. In (Watts et al. 1992), he not only discussed in detail the stability problems that Lyon had mentioned in his 1991 publication, but also elaborated on DR, matching and compactness; issues that were very superficially treated up to that point in time. Watts' improvements revolved around:

1. DR and stability: He found that by using one diode per side to degenerate the OTA, he could increase the input DR of the filter stage by 7.6dB. Moreover, by degenerating only the OTAs of the feed-forward path in Fig. 3, while keeping the feedback OTA narrow, he could eliminate the large-signal stability problem firstly addressed by Lyon one year earlier.
2. Improved Layout: Apart from applying obvious layout techniques like: a) making devices generally larger, b) placing match-sensitive devices close to each other and c) using common-centroid geometries, Watts realized that for a massively cascaded system such as the cochlea, one should work with the available chip area and mainly focus on the matching of critical devices. One example of his well-thought approach was the layout of the three transistors responsible for biasing the three OTAs in Fig. 3. Instead of duplicating each of the biasing transistors, laying them out in a hexagonal arrangement around a central point and connecting the pairs together in parallel, he realized that for equal capacitances in the filter, it was important only for the transconductance g_{mQ} to match the *sum* of the two feed-forward $g_{m\tau}$ transconductances and not the individual transconductances (see transfer function in Fig. 3). Thus, he duplicated only the feedback biasing transistor and juxtaposed that pair with the feed-forward biasing transistors in a 'pseudo-quad' formation as shown in Fig. 10. In addition, the initial Lyon cochlea relied on *identical tilts* on two resistive (polysilicon)

lines which set the voltages V_τ and V_Q to achieve uniform Q at each stage. In Watts' design, he used only one resistive line for both the τ and Q biasing transistors and controlled the actual Q value by changing externally the source voltage of the Q biasing transistor. In this way he was able to eliminate the mismatch for the case where two resistive lines were used and simplify considerably the actual testing procedure.

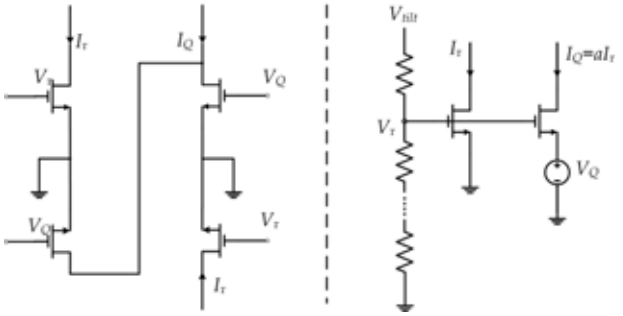

Fig. 10. The 'pseudo-quad' structure, formed by duplicating the Q bias transistor and juxtaposing the resulting pair with the τ bias transistors (left). Q-source control by externally providing a voltage V_Q to scale the feedback amplifier current I_Q with respect to I_τ (right); adapted from Watts (Watts et al., 1992).

3. Compactness: Apart from the careful layout, Watts also considered how to save space. In particular, he noticed that the first feed-forward OTA shared a common output node together with the feedback OTA. Thus, he eliminated two redundant transistors by sharing a single current mirror between the two OTAs. Lastly, he observed that while the output V_3 was a LP version of the input V_1, the output current of the feed-forward OTA was related to V_3 by $I_{OUT} = sCV_3$. Thus, there was no need to devote extra circuitry for the differentiator circuit to convert BM displacement to BM velocity (i.e. from LPF to BPF response).

As a final point, Watts was actually one of the first to comment on the overall power consumption of his chip (7.5mW/11μW for a 51-stage cascade with/without the circuits for making the results of the computation externally observable). Indicative measurements from his chip are shown in Fig. 12.

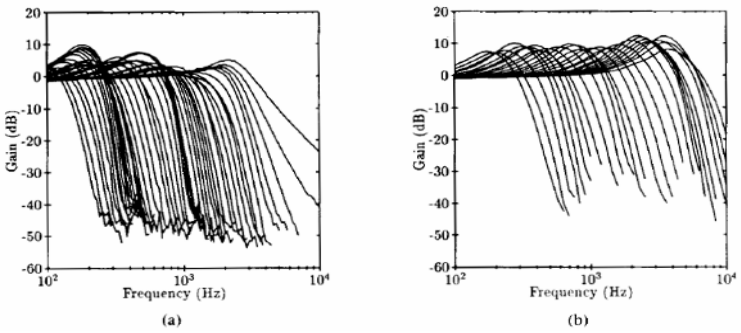

Fig. 11. Frequency response at each voltage tap. (a) Early layout. (b) Improved layout; from Watts (Watts et al., 1992).

Up to that point, it seemed that most of the development of analogue VLSI cochlea design was undertaken by the people at Caltech. From 1992 onwards, research contributions from other university groups started to arise. For example, a journal paper was published in 1992 by ***Weimin Liu*** and ***Andreas Andreou*** from Johns Hopkins University (Liu et al. 1992), where he presented an analogue CMOS implementation of a model of the auditory periphery; his neuromorphic effort was heavily influenced by Lyon's and Lazzaro's previous efforts and in certain aspects extended and improved their modelling work. Liu designed a complete system that included, apart from the BM and its transducers, the filtering effect of the middle ear. His BM model was Lyon's cascade/parallel model but the actual arrangement of the transfer functions was slightly different: he used simple (passive) first-order LP filters to form a 30-stage cascade with a BP biquad connected at each tap; all filters were g_m-C operating in WI. As with Lyon's initial chip, tuning was achieved by using two polysilicon resistive lines. Liu also built a separate chip containing the circuits of IHC and synapses (based on the neurotransmitter substance reservoir model (Smith and Brachman, 1982)) and provided similar measured results to Lazzaro's (i.e. BM-tap frequency response and auditory-nerve firing rates). Although Liu's effort was important in its own right, it did not advance the field by presenting results from a system with AGC or from a detailed performance assessment (he only reported on the 15μW power consumption).

An interesting circuit contribution came from ***Jyphong Lin*** the same year, who used switch-capacitor (SC) techniques to design the biquad filters employed in his cochlea model. As far as we know, that was the first non g_m-C-based cochlea design effort. Lin published two separate conference papers in 1992 (the first dedicated solely on the design of the SC cochlea filters (Lin et al., 1992b) and the second on the design of a SC filterbank (Lin et al., 1992a)) and a complete Journal article with measured results in 1994 (Lin et al., 1994). The designs of his SC biquads were area-efficient, because they were synthesized using the charge-differencing technique in which the time constants are controlled by both the product of capacitor ratios and the differences of the capacitor values, thus making the capacitor spread ratio small. His overall transfer function consisted of a cascade of two biquad filters; a LP together with a highpass (HP) response. The end result was an asymmetric BP shape similar to the one depicted in Fig. 2, with the added benefits (high precision and reliability) offered by the SC technique.

In his second conference paper, he designed a 32-channel filterbank to model BM filtering with each channel employing a 6^{th}-order asymmetric BP response. In filterbank architectures the input is applied to all channels simultaneously, whereas in a filter-cascade the input is applied serially and gets successively filtered before reaching each output tap (see Fig. 12). For this reason, Lin's particular choice of modelling BM filtering together with his chosen asymmetric BP response may be classified as bio-inspired and bio-mimetic but not neuromorphic. What made his contribution interesting is that he used a biquad sharing technique (Chang and Tong, 1990) to achieve an efficiency of computation without the associate disadvantages of the filter-cascade architecture (like instability, sensitivity to mismatch, noise and offset accumulation etc.). In his *dilating-biquad filterbank*, each channel output was formed by the addition and scaling of three BP biquad responses from three separate channels, thus facilitating considerable area savings. In other words, instead of using 192 biquads, he used 34 biquads and 32 sum-gain amplifiers; 66 in total (see Fig. 13). The only problem with this scheme is that the three dilated biquads must have constant Q values in order for the resulting higher-order response to maintain its shape and since all

biquads are inter-connected, the whole filterbank must be of constant Q. This is a significant drawback for applications where a realistic, OHC-based, AGC needs to be incorporated.

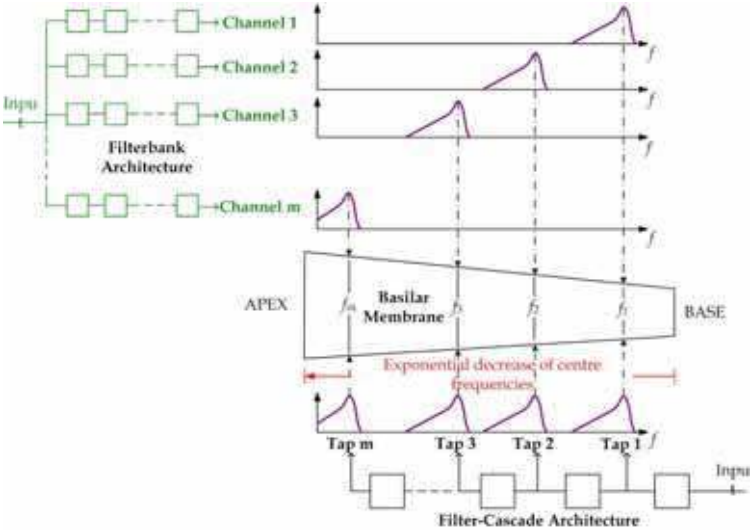

Fig. 12. Modelling BM filtering via neuromorphic (filter-cascade) and bio-inspired (filterbank) architectures.

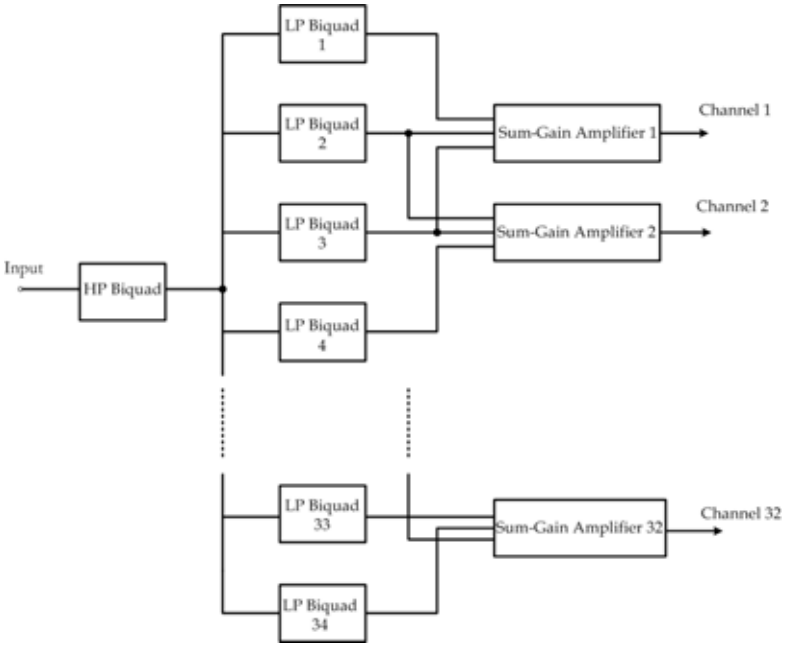

Fig. 13. Dilating-biquads filterbank; adapted from Lin (Lin et al., 1992a).

3. Increasing the performance: 1993 - 1998

1993 & 1994: After Lazzaro's work, the second sound localization systems were presented in 1993 and 1994 by ***Neal Bhadkamkar*** from Stanford University (Bhadkamkar and Fowler, 1993;Bhadkamkar, 1994). The 1993 effort was based on a design that was an architectural duplicate of the biological system (i.e. neuromorphic), whereas the 1994 effort was not, because it tried to duplicate some of the functions of the real system without relying on strict architectural analogies.

The neuromorphic system consisted of two fabricated chips; one chip contained the circuitry to model the left and right side cochleae, IHC and auditory neurons, whereas the other chip contained circuitry to model the binaural cross-correlation activity of neurons in the superior olive of the brainstem. Even though the system-level ideas were identical to Lazzaro's and Lyon's, Bhadkamkar's 1993 circuit design choices were slightly different. For example, Bhadkamkar's 1993 design included separate voltages to control the propagation delays and cut-off frequencies of the stages, respectively. This fact, together with his choice of a more complex transfer function for each BM section, resulted in a multiresolution BM design where the frequency resolution could be increased without excessively increasing the propagation delay[1] (Bhadkamkar, 1993). Similarly, the differentiator used for the IHC was different than Mead's hysteretic differentiator because it was designed to pump current into the SGN circuit during the discharge time of the capacitor. At low frequencies this occurred approximately half of every input cycle that it saw. At high frequencies, current was pumped in for a much smaller portion of the cycle. Thus, at these high frequencies, increases in the amplitude of an input sinusoid caused a sudden but temporary increase in the current that pumped into the SGN circuit. His SGN circuit was identical to Lazzaro's and Mead's but included a refractory period control i.e. freedom to control the time needed to elapse before permitting the SGN input current to have any effect. Moreover, his correlator chip was similar to that presented by Lazzaro, but his axons (delay-lines elements) received pulses in parallel and not serially to eliminate the accumulation of errors. Finally, no winner-take-all circuit was used; each output was summed together with the other corresponding outputs along all frequency channels and integrated using a leaky integrator.

On the other hand, his 1994 bio-inspired system was designed using two separate parallel banks of simple g_m-C BP filters. As mentioned previously this is not an accurate cochlea model but improves localization accuracy by removing the accumulation errors inherent in the cascade structure. The design of the IHC was based on a half-wave rectification, LP filtering and pulse-width modulation, with the pulse-width being a monotonic function of the amplitude of the LP-filtered, half-wave rectified signal. Thus, in this case he chose a pulse-width-modulation scheme for the neural encoding as opposed to the pulse-frequency-modulation used in his 1993 effort.

That same year the first current-mode cochleae designs arose; one from ***Christopher Abel*** (Abel et al., 1994) and one from ***Christofer Toumazou*** and ***Tor Sverre Lande*** (Toumazou et al. 1994). The former effort presented a novel implementation of a silicon cochlea based on

[1] One of the disadvantages of the cascade approach is that the propagation delay of the travelling wave from the input to a particular output tap is controlled by the same parameter that controls the cut-off frequency of the filters. This leads to the problem that the accumulated delay increases as a function of the number of filters per given frequency range, i.e. the larger the frequency resolution, the more the accumulated delay.

discrete-time, switch-current biquads. *Since the equivalent continuous-time cut-off frequency of a discrete-time filter is proportional to the sampling rate, reducing the sampling rate by a factor of two lowers the cut-off frequency by one octave.* Abel exploited this fact and realized that a set of filters designed to cover one octave may be used again at a reduced sampling rate to cover a lower octave. This technique allowed the entire range of audio spectrum to be covered by one repeated set of filters, thereby avoiding the need of a wide-range of integrator time constants and allowing for great area savings.

Abel's architecture is shown in Fig. 14. In addition, unlike SC, the switch-current technique does not require linear capacitors and produces filters that are thus compatible with standard CMOS digital processes. Abel's contribution was really interesting because he not only used a totally different circuit technique (let alone signal representation) to design his system, but also he showed preliminary simulation results from a very simple *Q*-control circuit. To avoid any confusion, Abel's *Q*-control circuit was not intended to close-the-loop between each stage of his cascade. By *Q*-control circuit he meant a circuit where adjustment of his biquads *Q* values could be possible, but this adjustment did not happen automatically according to signal strength.

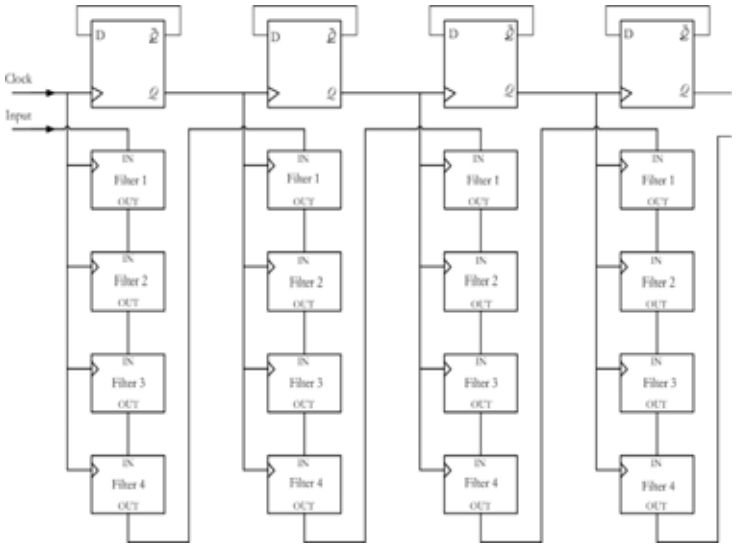

Fig. 14. The system level block-diagram of Abel's proposed design. A single D flip-flop acts to divide the clock frequency by two after each stage. This allows one set of four filters to cover multiple octaves; adapted from Abel (Abel et al., 1994).

Toumazou's contribution was quite substantial at the time. To this author's knowledge, his effort was the first *true* continuous-time current-mode implementation of a BM segment that employed the aforementioned companding technique (check Lyon's quote in 1991) to achieve high-DR and low-power dissipation. The companding strategy was based on the pioneering contributions of Douglas Frey (Frey, 1993;Frey, 1996)on the systematic synthesis of the so called *log-domain* filters published only a year before. The rationale behind this is that the signal is firstly compressed to an intermediate nonlinear voltage according to the logarithmic *I*-to-*V* relationship of WI MOS devices. The compression generally leads to

voltage swings that are small thereby allowing low-power operation. Also, through the application of the particular nonlinear compressive law, a wide range of signals could be accommodated at the input without needing to spend additional power (like in conventional g_m-C designs). After compression, the intermediate nonlinear voltage signal gets filtered and subsequently expanded at the output, using the exponential *V*-to-*I* relationship of WI MOS devices and thus maintaining overall input-output linearity. Because of the fact that the compression law is based on the natural logarithm, the resulting filters were called log-domain filters. Toumazou's design demonstrated a simulated input DR of 80dB, while dissipating a mere 125nW/pole. Toumazou's contribution was quite valuable at the time, because a) it revealed the potential of current-mode design within the particular cochlea application and b) it showed results from the 1st ever CMOS log-domain biquadratic filter.

1995 & 1996: Around 1995, papers that focused more on performance started to arise. ***Paul Furth*** and Andreou from Johns Hopkins University published three papers spaced one year apart. His 1995 effort (Furth and Andreou, 1995a) detailed the design of a multiresolution analogue filterbank with the primary engineering constraint being power consumption. He presented a design strategy for hardware cochlea filterbank models addressing issues both at architectural- and circuit-design level. Architecture-wise, Furth used a slight variation of Liu's filterbank (see 1992). In particular, Furth added two cascaded identical BP biquads at the output of each of the 16 taps to increase the per-tap selectivity much like what Liu did in his PhD dissertation (Liu, 1992). Furth was actually one of the first to address in more detail the DR problem with g_m-C designs. Instead of designing a linearized OTA (with a *tanh I-V* transconductance characteristic), he resorted to a CMOS Class-AB stage (with a *sinh I-V* transconductance characteristic) due to the facts that: a) it uses minimal number of components, b) it has a wide tunability range by tuning its supply voltages or substrate terminals and c) it contains no biasing elements, thereby rendering it the less noisy from all CMOS transconductor configurations at a given bias current (see Fig. 15). Furth consequently derived and numerically computed the maximum DR of a LP integrator employing two Class-AB transconductors. He showed that for a pure tone input, the maximum distortion-free DR (i.e. in which the distortion components equal the noise floor) is 44.3dB, whereas the maximum distortion-limited DR (for an output THD of 2%) is 49.4dB. He then estimated the distortion-limited DR at the output of each tap to be 28.2dB. The power supply of his circuits was 1.5V and the total power dissipation of a 16-tap filterbank was 355nW; the lowest reported up to that point.

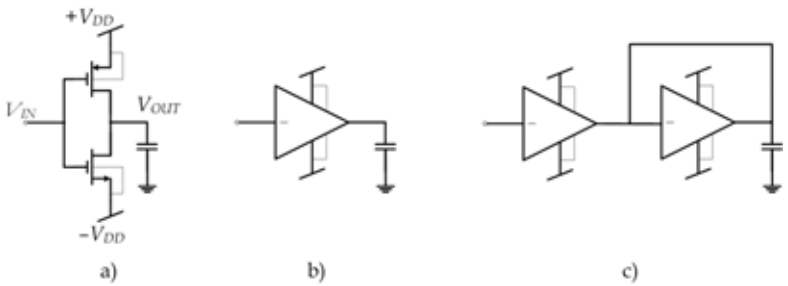

Fig. 15. a) the CMOS Class-AB transconductor, b) its symbol and c) the topology of a LP integrator; adapted from Furth (Furth and Andreou, 1995a).

In his 1996 effort (Furth and Andreou, 1996a), Furth took a different approach. He compared two differential-pair OTA employing respectively the single and double diffusive source degeneration technique (Boahen and Andreou, 1992). Circuit-wise the diffusor is a floating active MOS resistor placed in between the sources of a differential-pair. The diffusivity or conductivity of this resistor depends on the aspect ratio and it could be electronically controlled by varying the gate voltage. He found that the DR was 56.8dB for the single diffusion OTA (a 13.2dB improvement over the basic differential-pair) but extra common-mode circuitry was required. On the other hand, the double diffusor OTA exhibited 3dB less DR but without adding power or needing extra common-mode circuitry. Furth built the two OTA in a 2μm CMOS process using large device areas (1377μm/4.8 μm) and measured their relative DR performances, which came out being 10% lower than the aforementioned theoretical values. The diffusor source degenerated OTA with their corresponding *I-V* transconductance relations are depicted in Fig. 16. All parameters have their usual meanings, while *m* denotes here the aspect ratios of the diffusors.

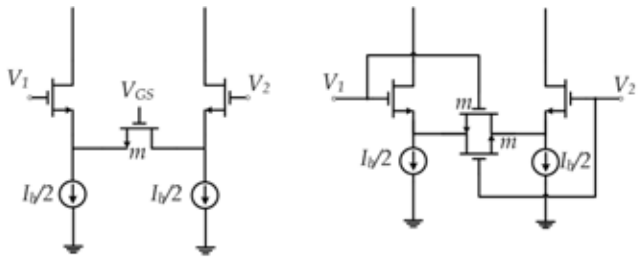

Single Diffusor: $$I_{OUT} = I_b \tanh\left[\frac{V_1 - V_2}{2nV_T} - \tanh^{-1}\left(\frac{\sinh\left(\frac{V_1 - V_2}{2nV_T}\right)}{2m + \cosh\left(\frac{V_1 - V_2}{2nV_T}\right)}\right)\right]$$

Double Diffusor: $$I_{OUT} = I_b \tanh\left[\frac{V_1 - V_2}{2nV_T} - \tanh^{-1}\left(\frac{1}{4m+1}\tanh\left(\frac{V_1 - V_2}{2nV_T}\right)\right)\right]$$

Fig. 16. Linearized OTA by means of single and double diffusive source degeneration; adapted from Furth (Furth and Andreou, 1996a).

In 1996, ***Jenn-Chyou Bor*** adopted the previous practice of other authors on SC filters and presented a SC cochlea cascade of 32 sections based on the transmission-line model of Zwislocki (Zwislocki, 1950). In essence, Bor resorted to the 2-D nonlinear partial differential equation describing the transmission-line cochlea model and by applying the principles of discrete-time signal processing and variable transformation, he reduced it into several 1-D equations that could be realized using circuits designed through the multiplexing SC technique. In his paper (Bor and Wu, 1996), he demonstrated through measurements a neuromorphic BM-cascade cochlea with very low sensitivity to process variations (see Fig. 17). The resulting filters operated from a ±3V supply and the single filter stage DR at 1KHz and 1% THD was measured 67dB (the highest reported up to that date). Bor also provided a table with the errors from the measured peak gains and peak frequencies (i.e. CF) from theoretical values. Yet, no IHC, neuron or OHC-based AGC circuits were designed.

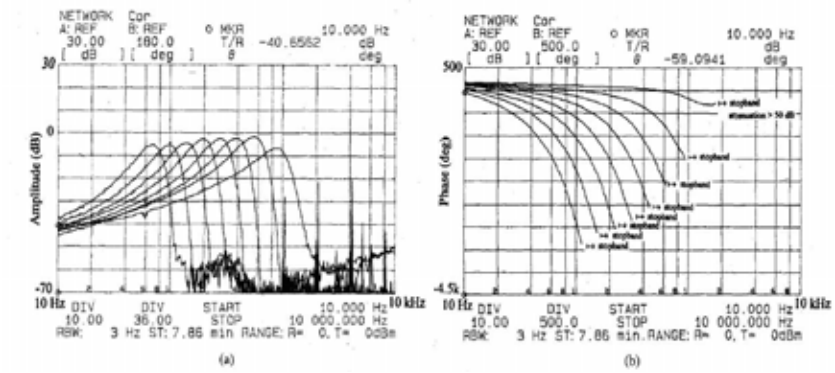

Fig. 17. Measured a) amplitude and b) phase responses from 8 taps of a 32-section SC filter-cascade; from Bor (Bor and Wu, 1996).

Within Carver Mead's group, ***Rahul Sarpeshkar***, the successor of Watts, took the rather challenging direction of designing a high performance neuromorphic cochlea cascade. As mentioned previously, the group's prior g_m-C biquad designs had their large-signal stability limit smaller than their small-signal stability limit. This misbehaviour forced them to set the gains, for each stage of the cascade, at conservatively small values (i.e. having very low Q) in order to ensure that each stage remained stable at large signal levels. Consequently, this resulted in small pseudo-resonant peak gains (around 12dB in (Lyon and Mead, 1988a)) and input DRs between 20 – 40dB at best. Initially, Sarpeshkar focused on the careful design of the OTAs comprising the biquads and in (Sarpeshkar et al., 1996) he designed a wide linear range OTA (named the WLR) through the use of four linearization techniques extending the linear range from 75mV to 1 – 1.75V. With Fig. 18 as a reference, these linearization techniques were:

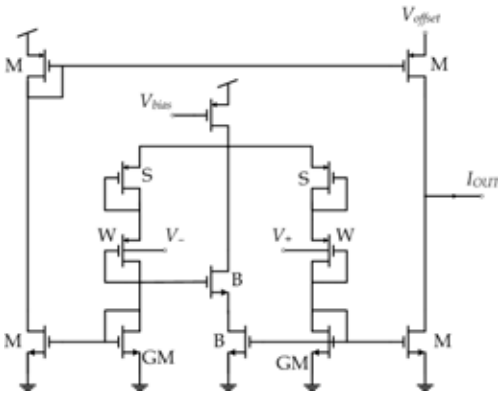

Fig. 18. The WLR OTA. The devices marked S and GM denote the source and gate degeneration transistors, whereas the devices W and M denote the well-input and mirror transistors. The B transistors perform bump linearization. In addition, the voltage V_{bias} sets the bias current of the amplifier, whereas V_{offset} allows fine adjustment of the amplifier's output offset if necessary; adapted from Sarpeshkar (Sarpeshkar et al., 1996).

1. Instead of using the gates of the W devices as inputs he used their wells due to the well's lower transconductance. To avoid latch-up he used large common-mode voltages in the range 1 – 5V.
2. Devices S lower the transconductance of the W devices further through the common technique of source degeneration.
3. Devices GM lower the transconductance of the W devices even further through gate degeneration. An increase in current in either of the two differential pair branches causes an increase in voltage of the GM devices that is fed-back to the gate of the W transistor and turns it off.
4. Bump linearization. The bump circuit was proposed by Delbrück in (Delbruck, 1991) and the way it linearizes the *tanh* function of an OTA is qualitatively similar to Katsuji Kimura's triple-tail technique (Kimura, 1995). The basic idea of the bump transistors is that they steal current from the two branches of the differential pair at low differential voltages, thereby reducing the transconductance. Moreover, by appropriately choosing their aspect ratios, odd-order harmonic distortion gets suppressed as compared to the tailor expansion of the standard *tanh* characteristic.

Sarpeshkar then incorporated the WLR to create biquad filters forming a 45-stage BM cascade. His filter design (a block diagram of which is shown in) was based on that of Fig. 3 but with the following three modifications:

1. Since the well was used as the input, there were no explicit capacitors in the filter topology; he used the well capacitance. In addition, since the well-to-bulk reverse bias voltage was of the order of 3V, this capacitance was fairly constant without introducing excessive distortion at the output.
2. The feedback OTA (amplifier A_3 in Fig. 3) now implemented a non-monotonic function with a fuse-like characteristic. Recall that Watts was the one who linearized OTAs A_1 and A_2 while leaving A_3 narrow to eliminate the large signal instability. Sarpeshkar, on the other hand, linearized OTAs A_1 and A_2 and made the characteristic of A_3 to as such so that positive-feedback amplification shunts-off completely instead of simply saturating at large signal levels. Thus, at high-levels it effectively reduces the gain of the stage resembling the compressive mechanisms attributed to OHC operation. In essence, the fuse-like OTA performed static nonlinear compression. Note that OTAs with fuse-like characteristics where presented earlier in (Kimura, 1994).
3. Finally, he followed Watts' ideas on compactness and realized that the feedback fuse-like OTA shared the same differential inputs as the output feed-forward OTA and the same output as the first feed-forward OTA. Thus, he shared their differential pair and output mirror circuits, allowing the fuse-like OTA to be implemented by only four transistors.

Sarpeshkar's 1996 effort formed the basis of his forthcoming complete design presented two years later. His architectural and topological choices gave rise to biquad filters that exhibited input DR in excess of 60dB i.e. an order of magnitude larger from the group's previous g_m-C efforts. However the topology shown in Fig. 19 had a very specific drawback; *the noise per unit bandwidth increased with Q*. This was because in that particular biquad topology, the Q was obtained through the addition of positive-feedback currents (marked I_{fb} in Fig. 19) which contributed additional shot noise. As it will be shown later on, his 1998 effort employed a different biquad topology (based on the DIFF2 structure which was discussed by Lyon in 1992 (Lyon, 1991)), although the WLR topology remained the same.

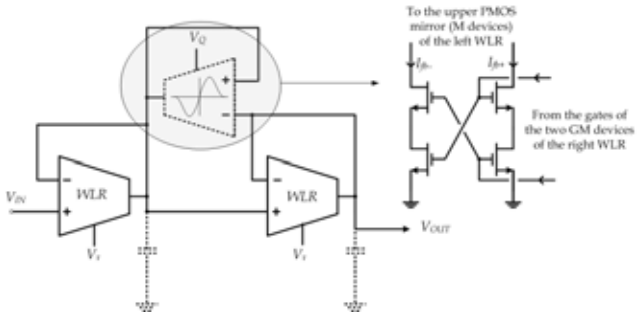

Fig. 19. A schematic block diagram of the fuse biquad. The dotted components indicate that they are not explicitly implemented in the actual circuit topology. The voltages V_τ and V_Q set the pole frequency ω_o and quality factor Q of the filter; adapted from Sarpeshkar (Sarpeshkar et al., 1996).

In the same year, ***Andre Van Schaik*** from EPFL's MANTRA Center for Neuromimetic Systems, together with ***Eric Vittoz*** addressed in detail the problem of matching in CMOS WI for the second time since Watts's 1992 effort (A.Van Schaik et al., 1996). Van Schaik used Compatible Lateral Bipolar Transistors (CLBTs) in a 104-stage cochlea cascade, to create the exponentially scaled currents when biased with a resistive line with a linear voltage gradient between its two ends. CLBTs can easily be made in a CMOS substrate and contrary to simple WI MOS devices, their collector current is *independent* of the CMOS technology's threshold voltage. The remaining mismatch is due to the geometry mismatch of the devices, but this parameter is much easier controlled than the variance of the threshold voltage. A CMOS CLBT can be obtained if the drain or source junctions of a MOS device gets forward-biased in order to inject minority carriers to the local substrate. If the gate voltage is negative enough (for an n-channel MOS) then no current flows at the surface and the operation is purely bipolar (Vittoz, 1983). A diagram showing the carrier flow and bipolar operation of a MOS transistor is shown in Fig. 20.

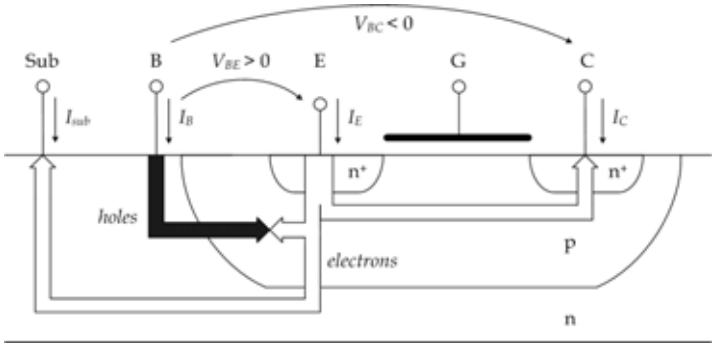

Fig. 20. Bipolar operation of a MOS device; adapted from Van Schaik (A.Van Schaik et al., 1996).

Much like Watts, Van Schaik identified that the biquad's biasing transistors (i.e. those that set the pole frequency and Q) had to be precisely matched. In prior designs, these transistors were simple MOS, thus a small variation in their threshold voltage would result in a large

variation in their output current due to the (inherent in WI) exponential *V*-to-*I* relationship. CLBTs offered a considerable improvement in the regularity of the frequency spacing of the cochlea filters which is of significant importance to long filter-cascade models, since one filter can distort the input signal for all the subsequent stages. Results showing the cascade's improved frequency response and spacing regularity are shown in Fig. 21. Finally, in 1996 Van Schaik published together with ***Ray Meddis*** an article describing preliminary designs of IHC and SGN circuits (van Schaik and Meddis, 1996) which were used later by the author in forthcoming publications.

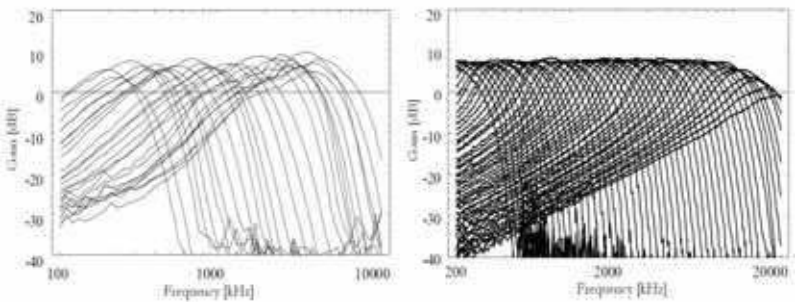

Fig. 21. Comparison between the 1992 design of Watts (left) with the improved design employing CLBTs (right); from Van Schaik (A.Van Schaik et al., 1996).

1997: As mentioned previously, ***Furth*** published his third paper in 1997 (Furth and Andreou, 1996b). Following Sarpeshkar's 1996 work on increasing the OTA linear range, that particular effort varied along the same lines and presented a new wide linear range OTA. Furth's OTA topology was based on the initial BiCMOS design of Liu and Andreou (Andreou and Liu, 1992) which incorporated an OTA operating in strong inversion, a bipolar Gilbert multiplier cell and a WI MOS current buffer. Liu claimed that the choice of the two different modes of operation together with the individual optimization of each block could lead to an increased overall performance regarding power consumption, DR, tuning range and area. In this effort, Furth made some modifications to Liu's and Andreou's design by linearizing the OTA by means of a double diffusor and by replacing the Gilbert multiplier cell by a WI MOS equivalent. In this way the problems associated with beta reductions, beta mismatch and/or large leakage currents of the bipolar devices could be alleviated. His simulations yielded a linear range of ±260mV and an estimate (based on an empiric choice of noise floor value) for the DR of 66dB. His OTA design is shown in Fig. 22.
One of the better contributions in analogue VLSI cochlea modelling came the same year from ***Eric Fragniére*** with ***Van Schaik*** and ***Vittoz*** (Fragniere et al., 1997). Together they proposed an analogue VLSI model of an active cochlea based on Lyon's silicon BM filtering implementation. Circuit modelling-wise they exploited the same g_m-C biquad design as the one proposed by Lyon and Watts in 1992 (i.e. the one with the two feed-forward OTAs degenerated with one-diode per side, while keeping the feedback OTA narrow), but they also provided a thorough analysis (with CMOS WI circuit implementations) on an adaptive AGC scheme for regulating the stages *Q* values that was never reported before.
They implemented a *feedback closed-loop* AGC scheme, where the signal at an output tap is used to regulate the *Q* of a specific preceding stage according to *a square-root level compression law* (and not a linear one like Hirahara presented in 1989). From their study they

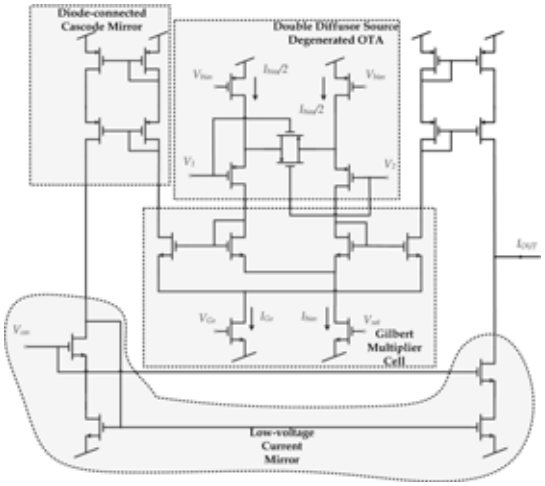

Fig. 22. Furth's wide linear range OTA implementation. The voltage V_{Go} sets the gain of the Gilbert Multiplier Cell, V_{sat} is the biasing of the level shifter transistor, whereas V_{cas} is the biasing of the low-voltage current mirror; adapted from Furth (Furth and Andreou, 1996b).

realized that in order to locally control the pseudo-resonant gain at the output of a particular stage, only the Q of the stages participating to the build up of that pseudo-resonance had to be controlled. Their findings can be summarized in the following sentence: '*The output from any stage in the cascade must control the Q of a stage located at a basal distance corresponding to a CF increase between one sixth and one third of an octave from that particular stage's output*'. This conclusion was supported by physiological evidence which revealed that afferent fibres of IHC are paired with the afferent fibres of OHC located at one seventh to one third of an octave higher CF (Kim, 1986). In other words, they not only specified the law with which the output-tap's signal level was mapped to the stage Q values, but they also provided a design framework for *distributing* the gains along the cascade. Fragniére's per stage local feed-back AGC scheme is shown in Fig. 23. The V_{din} is the voltage output from the previous stage, whereas V_{dout} is the output voltage representing BM displacement of the current stage. Following Watts observation on compactness (see 1992), I_{vout} is a current signal representing BM velocity (i.e. it is the differentiation of V_{dout}) which consequently passes through a half-wave rectifier representing the action of the IHC. The output from the rectifier goes to a mean spiking rate (MSR) lossy integrator that computes the mean value of the half-wave rectified I_{IHC}; the output of the MSR (i_{IHC_DC}) is a quasi-DC signal that represents signal strength. The final stage is the Q decision block (implemented by means of a simple WI translinear loop) that maps I_{IHC_DC} to the correct $I_{t\tau}$ and I_Q values that set the ω_o and Q of the filter. With Fig. 3 as a reference, the Q decision circuit implements the following control law:

$$Q \propto \left(\frac{g_{mQ}}{g_{m\tau}}\right) \Rightarrow \frac{I_Q}{I_\tau} = \left(\frac{I_{Q\max}}{i_{IHC\_DC} + I_o}\right),$$

where I_{Qmax} corresponds to the maximum Q value for zero input, I_o is a DC level ensuring loop stability for zero input and with I_Q varying geometrically with signal strength implying a logarithmic compression-type mapping.

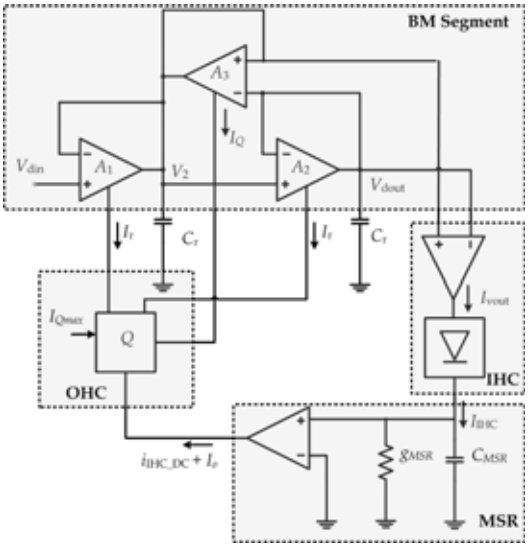

Fig. 23. Analogue model of one stage of the active cochlea cascade; adapted from Fragniére (Fragniere et al., 1997).

Finally, it should be mentioned that all the results shown in this work were simulated using mathematical software tools like MatLab and not from detailed circuit simulations or measurements. For this reason, Fragniére's contributions are considered significant but from the overall system-level modelling perspective and less from a circuits or performance evaluation perspective.

1998: Even though seventeen years had passed from Lyon's initial 1981 paper, still no publications detailing measured results from an 'active' silicon cochlea existed. Fragniére's efforts were indeed influential, but still his modelling ideas had to be demonstrated in an actual analogue hardware realization. *The most complete single-piece of work on a neuromorphic silicon cochlea came in 1998 by* ***Rahul Sarpeshkar*** *from Carver Mead's lab*. In (Sarpeshkar et al., 1998), he described an 117-stage, 100Hz-10kHz, silicon cochlea that attained a DR of 61dB (at 4% THD) at the CF of a typical stage while dissipating 0.5mW of static power, by using the following techniques:

1. A modified version of the previously described WLR. Here he did not use source degeneration as in the design of Fig. 18, but used cascode circuitry to increase the DC gain and prevent low-frequency attenuation in the cochlea.
2. An improved biquad filter topology that is low-noise by overcoming the problem of his previous 1996 topology where the output noise scaled with Q.
3. DR gain control through a local, fast-acting *feed-forward* AGC. Architecture-wise Sarpeshkar's AGC loop is the same as Fragniere's but acts on the level of the stage's input and not output.
4. Automatic offset-compensation circuitry in each cochlea stage prevented offset accumulation along the cochlea cascade.
5. The architecture of three, overlapping 39-stage cochlea cascades (see Fig. 24). In this architecture the input is fed in parallel to tiny cochlea cascades whose corner frequencies overlapped by 1 octave. This particular architecture may be viewed as a

hybrid of an architecture that has many parallel filters in a filterbank and one that has one filter-cascade with all filters in serial. Even though he partly deviated from a purely neuromorphic BM structure, he showed that by adopting this scheme he could reduce the group delay of his silicon cochlea and limit the accumulation of the $1/f$ noise.

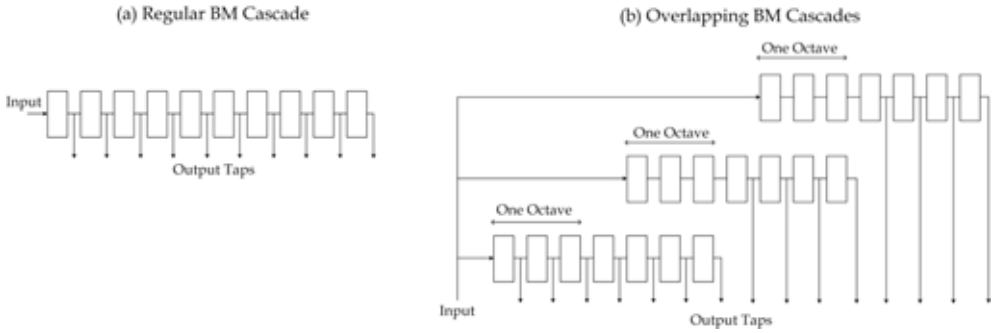

Fig. 24. Architecture of overlapping cascades. (a) In a standard filter-cascade the input is fed serially to all the stages, whereas in (b) the input is fed in parallel to tiny cochlea cascades that overlapped by one octave; adapted from Sarpeshkar (Sarpeshkar et al., 1998).

Moreover, Sarpeshkar presented a thorough evaluation of his system by presenting an arsenal of performance-related results like: amplitude and phase frequency responses, adaptation with/without AGC, harmonic-distortion levels at various taps, noise and distortion spectrums, spatial characteristics, etc. Finally, he provided insightful discussions on the comparison between his analogue CMOS WI implementation with a custom digital ASIC and on filter-cascade versus bandpass filterbank architectures. Sarpeshkar was able to demonstrate in silicon a variety of physiologically obtained results:

1. The frequency-to-place transformation as implemented by the amplification and propagation of travelling waves in the BM (much like the results of Fig. 4).
2. A compressive nonlinearity at and beyond the CF of a cochlea tap due to the dynamic and compressive action of the AGC with asymmetric attack and release responses to transient inputs.
3. Extension of the DR from 30dB to 60+dB due to adaptation and active amplification.
4. Sharp roll-off slopes (corresponding to 10^{th}- to 16^{th}-order transfer functions), broadening of the frequency response and shift of the CF towards lower frequencies as input intensity is increased.
5. Masking of adjacent frequencies and harmonics due to the distributed nature of his AGC and compressive nonlinearities.

In conclusion, Sarpeshkar's 1998 effort remains to this day one of the most complete neuromorphic cochlea designs. His contributions demystified the silicon cochlea operation, made a clear link to all the modelling ideas Lyon had presented in the past and advanced the neuromorphic field with performance figures that serve to this day as benchmarks to future design efforts.

The other two 1998 contributions came from ***Timothy Edwards*** and ***Nagendra Kumar*** from the Johns Hopkins group. Edwards' work presented the second log-domain biquadratic filter implementation for audio frequency applications since Toumazou's 1994 effort (Edwards and Cauwenberghs, 1998). The BP transfer function was realized by using two

integrators (one lossy and one lossless) with additional translinear loops to implement the feed-back gains. The overall design was BiCMOS and operated in Class-A. He also provided measured results regarding ω_o and Q frequency response tunability from a 4th-order BP response. Yet, no noise or linearity results were reported. On the other hand, Kumar's work was one of the first attempts to apply a bio-inspired system to speech recognition experiments (Kumar et al., 1998). Kumar adopted Liu's proposed filterbank architecture and he consequently implemented it using Furth's linearized WI OTA presented in (Furth and Andreou, 1995b). In addition, due to its physiological plausibility, power signal processing capabilities and relative noise immunity, he used a zero-crossing-based signal representation for abstracting the auditory nerve fibre responses. Thus, his 15-channel filterbank chip essentially computed zero-crossing intervals and signal energies in frequency sub-bands. He consequently reported on speech recognition results using the TI-DIGITS spoken digit database obtained from software simulation of the chip feature extraction algorithm.

3. Recent years: 1999 - 2008

1999: During 1999 there were two current-mode contributions; one from *Todd Hinck* and one from *Timothy Edwards*. Hinck's work was based on a current-mode implementation of the travelling-wave amplifier (TWamp) cochlea model. This model was proposed in 1993 by Hubbard (Hubbard, 1993) who hypothesized the existence of two separate wave-propagation modes in the cochlea. The TWamp model was realized using two actively-coupled transmission lines, each of which represented a different mode of energy propagation in the cochlea. The first transmission line was the same as in the classical travelling-wave model, whereas the second was composed of sections of a series inductor with a parallel shunt capacitor and resistor. Hinck's design strategy was quite similar to the one reported from Bor in 1996; He started from the transmission-line model of a BM segment Δx, he consequently converted it to a signal-flow-graph (SGF) and then replaced the SFG with current-mode equivalent blocks (i.e. gain and integrator blocks). In (Hinck et al. 1999), he showed simulation results from the frequency response of a 100-section cochlea with fixed Q and estimated the DR to be 54dB assuming a 100pA noise floor.
Finally, Edwards outlined the design of a current-mode filterbank front-end with signal feature extraction for acoustic pattern recognition using his 1998 work on log-domain filters (Edwards and Cauwenberghs, 1999). His feature extraction algorithm was based on rectification followed by smoothing and peak detection and tracking for which he showed current-mode circuits. He provided measured results from a 15-channel (each channel comprising two cascaded log-domain BP biquads) chip built using the 1.2μm BiCMOS process with a measured DR of 35dB and a power dissipation of 200μW from a 5V supply. Moreover he was able to demonstrate that the action of the peak detector helped to increase the sharpening of the BP response (much like the difference in sharpening between the BM-velocity and neural tuning curves observed in the biological cochlea), compensating for the swallow low-frequency roll-off slopes typical of Class-A log-domain BP filters (see Fig. 25).
2000: In 2000, the first current-mode cochlea implant (CI) prosthesis system was presented by *Walter Germanovix* and Toumazou from Imperial College London (Germanovix and Toumazou, 2000). The function of a CI is to bypass the natural transducers (i.e. the IHC) which are damaged or missing in a diseased cochlea and consequently excite the SGN (via electrical stimulation) leading eventually to hearing perception. The proposed CI design was

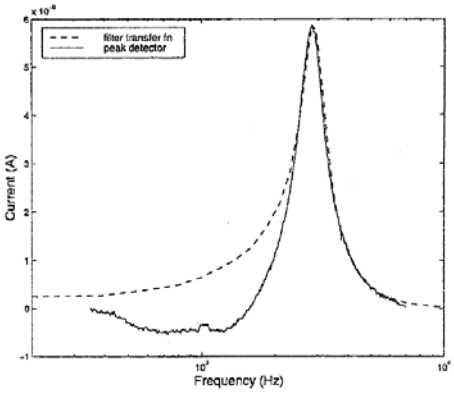

Fig. 25. Comparison between the measured transfer function of the BP filter of a single channel (dotted line), normalized to the current output of the peak detector and smoothing filter on the same channel (solid line); from Edwards (Edwards and Cauwenberghs, 1999).

switchable into two modes of operation: the single-channel and multi-channel modes. Single-channel CIs code frequency based on the rate of firing of electrical pulses, whereas multi-channel CIs use the place theory for coding frequency (i.e. the fact that different frequencies map at different places along the BM). Also, single-channel CIs usually employ the CA (Compressed Analogue) stimulation strategy, whereas multi-channel CIs employ the CIS (Continuous Interleaved Sampling). In the latter, each of the channels BP filtered envelopes of the input signal are encoded into non-overlapping biphasic electrical current pulses in order to eliminate any overlap between channels so that only one electrode is stimulating at a time.

Although multi-channel CIs are the prevailing devices around the world today, there are some arguments against the rational for their use. However, the cochleae of people with severe hearing impairment do not posses sufficient residual neuronal population to use tonotopic electrical stimulation through multiple electrodes. Therefore, there are arguments against the rational for using tonotopic stimulation strategies since multi-channel electrode systems aim to stimulate focal regions of dendrites along the BM, which might not exist in some/most cases (Namasivayan, 2004). For this reason, Germanovix attempted to create a versatile CI employing both aforementioned modes and stimulation strategies. The block diagram of his system is shown in Fig. 26.

One important feature of Germanovix' CI was the tone control circuit that follows the transconductance amplifier (OTA) in Fig. 26. The OTA (a simple *tanh* characteristic) was used to provide compression and sensitivity by converting the (wide) input DR (by varying its tail current) into an appropriate DR for the specific individual. Consequently, the tone control circuit allowed boost/cut of low/high frequencies to compensate deficiency in the diseased auditory system. The tone control circuit output was formed by subtracting the outputs of two parallel LP log-domain filters; one with low-frequency cut-off to emphasise the bass and one with high-frequency cut-off to emphasise the tremble. The operation of the tone control circuit is essentially similar to the bass/treble control of a Hi-Fi system. Even though Germanovix' contributions were only preliminary at the time, implementation-wise all his circuits were designed in CMOS WI, they were operating in the current mode and his BP sections were Class-A log-domain filters with a measured THD of –40dB (i.e. 1%) at a modulation index of 35%. No noise floor and power consumption figures were reported.

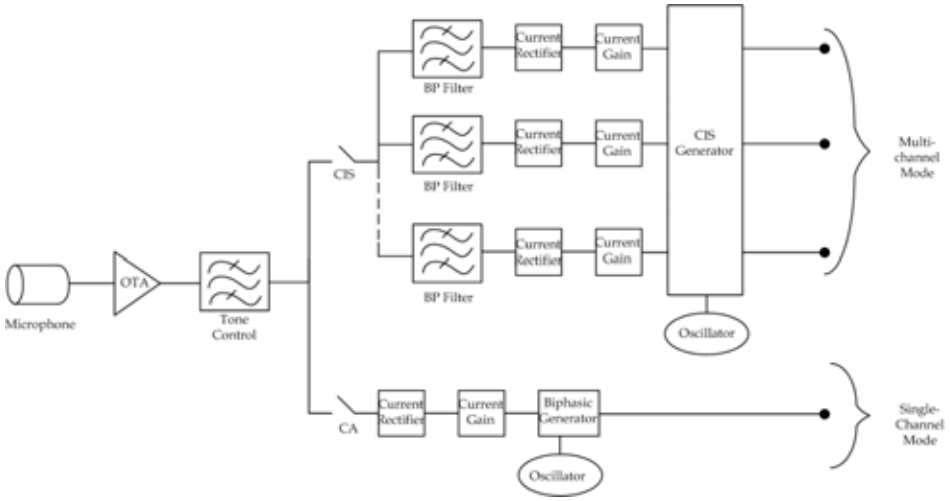

Fig. 26. Diagram of Germanovix' CI with switches between the CIS and CA modes of operation; adapted from Germanovix (Germanovix and Toumazou, 2000).

2001: In 2001 there were two contributions from ***André Van Schaik***. In the first one (Schaik, 2001), he presented an electronic system that extracted the periodicity of a sound. The system was comprised from three analogue VLSI building blocks: a) an improved version of Watt's 1-D implementation utilizing 104 cascaded sections (the same g_m-C ones that Watt's used in (Watts et al., 1992)) with CLBTs for generating the biasing currents (built on a 4.77mm × 3.21mm die chip), b) four IHC circuits (built on a 1mm² chip) and c) two spiking neuron chips (each chip built on a 2.5mm² and containing 32 neurons). Before explaining how his system performed periodicity extraction, let us briefly describe Van Schaik's IHC and neuron circuits, the initial versions of which were previously published by the author around 1996 (Van Schaik and Meddis, 1996).

His IHC circuit is the most bio-plausible contribution to date because it did not solely rely on half-wave rectification (like in all previous efforts) but attempted to replicate several other IHC characteristics/functions like input-output function asymmetry, temporal adaptation to constant stimulation etc. To appreciate Van Schaik's modelling choices, recall four interesting features of the biological auditory neuron fibre:

1. The spike rate of most auditory neuron fibres increase with increasing stimulus level but only over a narrow level of signal intensities (from 60 to 80 SPL). Above that level, the output saturates showing little or no further rate increase (see Fig. 27(left)). Moreover, the relation between the IHC cilia deflection and the percentage of open ion channels (or equivalently the IHC current to IHC membrane potential) has a sigmoidal form with a certain offset, so that only 20% of the channels are open at equilibrium.
2. The rate of firing is known to adapt to a new stimulus. The high rate at onset is quickly adapted to a lower rate within 3msec of the initial stimulus onset. In addition, when a persistent stimulus is present, the rate reduces even further but at a much slower pace (see Fig. 27(middle)).
3. IHC perform some kind of LP filtering with a cut-off frequency of 1kHz so that AC components of frequencies above about 4kHz are heavily attenuated and thus no information is available to the brain regarding the temporal properties of the input

waveform. At frequencies well below 4kHz, the IHC voltage has a noticeable AC component and its temporal structure can be extracted by the brain.

4. At low frequencies (< 3kHz) the spike rate in an individual auditory neuron can be shown to be a half-wave rectified waveform (see Fig. 27(right)). In the absence of any input signal, the auditory neuron shows spontaneous action potential at a frequency almost as frequent as half of the maximum firing rate.

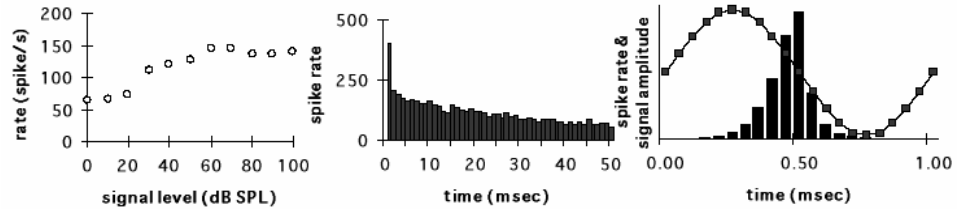

Fig. 27. (left) IHC rate-intensity function, (middle) IHC post stimulus time histogram showing adaptation to a persistent stimulus and (right) IHC period histogram shown with stimulating sinusoid; from Van Schaik (Van Schaik and Meddis, 1996).

Van Schaik's IHC model (shown in Fig. 28) consisted of three main processing stages that aim to model the four aforementioned features of an auditory neuron fibre: The first stage contained an asymmetric (sigmoid-like) compressive input-output function (realized by a simple OTA where one differential-pair transistor was 20% larger than the other – thus only 20% of the biasing current will flow through the smaller device when the input differential voltage is zero) followed by a bias circuit which adds bias to the membrane potential to guarantee spontaneous activity at the absence of any input (points 1 and 4). The second stage consisted of two first-order LP filters with a cut-off frequency of 1kHz or lower (point 3) and the final stage introduced adaptation to constant stimulation by subtracting a weighted LP filtered copy of the IHC output with the IHC output itself. By using a larger capacitor in the second filter (i.e. $C_2 = 3C_1$), its output will react more slowly to an onset of I_{sig} than I_1 would do (point 2). The final output current is given by $I_{out} = I_1 - GI_2 + I_{spont}$, where G (< 1) is the gain of the current mirror that controls the ratio of the system's peak response to the sustained response and I_{spont} is a constant current level used to adapt the 'spontaneous' rate of firing (point 4).

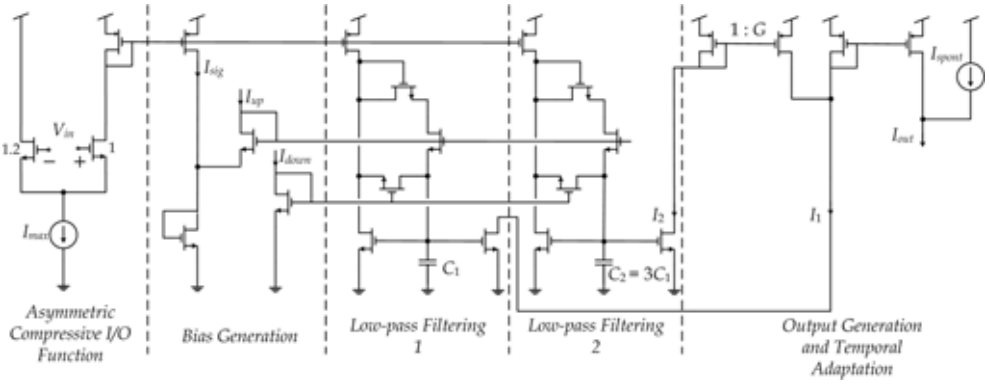

Fig. 28. Circuit diagram of the IHC stage; adapted from Van Schaik (Van Schaik, 2003).

Implementation-wise, one of the main problems/challenges in modelling comparatively slow brain elements with analogue VLSl circuits is the realization of large time constants such as the ones for the IHC LP filtering. Van Schaik realized that since the linearity of the LP filter stage is not an important issue, large time constants could be realized using the current mirror arrangement of the two LP filter blocks in Fig. 28 (i.e. small capacitors appear larger via the Miller effect). This current mirror creates a non-linear LP filter for which I_{up} sets the maximum rise speed and I_{down} sets the maximum fall speed of the voltage on the two capacitors. This construction allowed Van Schaik to obtain programmable time constants in the order of several milliseconds using capacitors in the pico-Farad range while using bias currents in the 100pA range. Moreover the time constants varied with input signal level for both the LP filter and adaptation stages. Fig. 29 shows a comparison of the output responses from his artificial IHC circuit relative to the biological ones. Clearly, Van Schaik's neuromorphic IHC circuit is able to faithfully reproduce the responses of its biological counterpart.

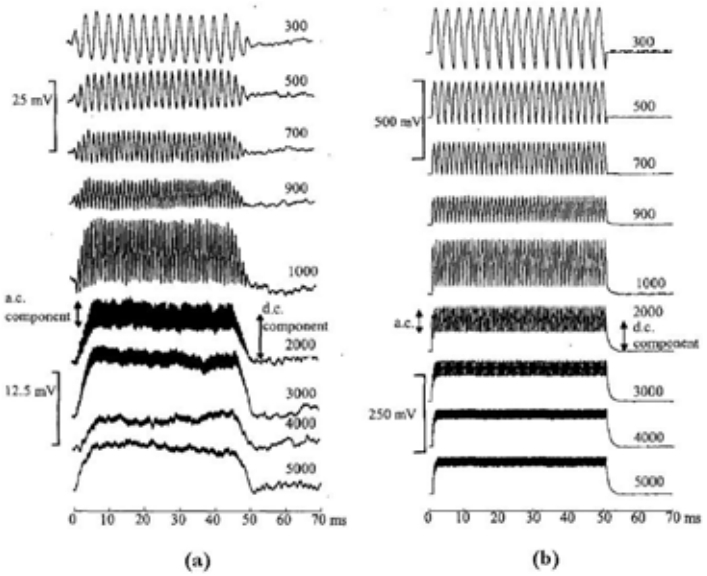

Fig. 29. Intracellular IHC voltage changes in (a) the biological IHC and (b) Van Schaik's circuit implementation for different frequencies of stimulation. For both cases, note the change of scale for the lower five traces; adapted from Van Schaik (van Schaik, 2003).

The final circuit was a silicon neuron (depicted in Fig. 30 above) which was designed after its biological counterpart. Recall that in the real neuron an increased sodium conductance creates the upswing of spike (i.e. activation through depolarization) and the delayed blocking of the sodium channels plus delayed increase of potassium conductances create the downswing (i.e. de-activation through re-polarization). Here, the membrane of the neuron was modelled by the membrane capacitance C_{mem} and the membrane leakage current is controlled by the current I_{leak}. In the absence of any input (i.e. I_{ex} = 0) the membrane (V_{mem}) potential is drawn to its resting potential controlled by V_{-}. Excitatory inputs add charge to

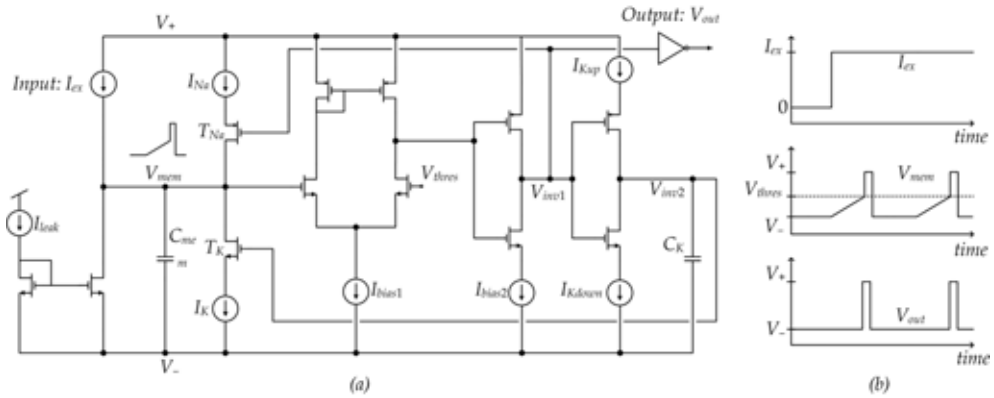

Fig. 30. (a) Circuit details of the VLSI neuron. (b) Example of the response of the membrane potential (V_{mem}) and the output signal (V_{out}) to a DC input current (I_{ex}); from Van Schaik (Schaik, 2001).

C_{mem}, whereas inhibitory inputs discharge C_{mem}. If the excitatory input (I_{ex}) becomes larger than I_{leak} then V_{mem} will rise from its resting potential. V_{mem} is then compared with a controllable threshold voltage (V_{thres}), using an OTA driving a high-impedance load. If V_{mem} is larger than V_{thres}, then the output of the OTA (V_{comp}) will be high and thus the output of the first inverter (V_{inv1}) will go low activating the PMOS T_{NA} switch which injects 'sodium' current to C_{mem} effectively pulling V_{mem} up (i.e. the upswing of a spike). At the same time, a second inverter has it output voltage (V_{inv2}) high allowing the capacitor C_K to be charged at a speed which is controlled by I_{Kup}. As soon as the voltage on C_K goes high, the NMOS T_K switch conducts allowing for the 'potassium' current I_K to discharge C_{mem} and bring V_{mem} down to its resting value. The values of the currents I_{Kup} and I_{Kdown} control the spike width and the neuron's refractory period respectively.

Van Schaik consequently used his improved BM cascade, IHC and neuron circuits to model periodicity extraction much like what Lazzaro had proposed and demonstrated in (Lazzaro and Mead, 1990). A major disadvantage of Lazzaro's implementation was the fact that in order to perform the matched filtering operation at the output of each SGN, each delay associated with a BM tap had to be matched precisely to the inverse of the CF of that tap. That meant that for a BM cascade whose CF changed exponentially from 4kHz to 100Hz, delays from 0.25msec to 10ms had to be created. In the real cochlea these large variations in delay is unlikely to be provided by an axonal delay circuit because it would require a very large variation in axon length. Van Schaik observed that the phase of a pure tone of a given frequency on the BM increases from base to apex and the phase changes rapidly around the CF. Moreover, the filter cascade acts as a delay line and each filter adds a delay which corresponds to $\pi/2$ at the cut-off of that stage. *Thus, if one monitors the output of filter i and filter i – 4, under the assumption that the cut-off frequency remains fairly constant between these four stages (i.e. for a high resolution BM cascade), then the delay would correspond to 2π at the cut-off frequency.* In essence, Van Schaik used the inherent delay of the BM cascade to perform the matched filtering operation at the output of the SGN and not through an additional axon circuit like Lazzaro. Van Schaik demonstrated through measurements that detecting these coincidences can yield very selective filters, i.e., filters responding only to a very narrow range of periodicities, but at the same time still responding after a few periods of the input

signal. This turned out to be an advantage over traditional BP filters, where an increase in selectivity has to be traded off against a decrease in response time.
Van Schaik's second 2001 contribution (together with Fragniére) detailed the analogue current-mode VLSI implementation of a 2-D cochlea model using a grid of transistors to model cochlea fluid mass (Van Schaik and Fragniere, 2001). That particular model was based on the initial 1992 2-D model of Watts that was thoroughly investigated by Fragniére in (Fragniere, 1998) few years later. The two dimensions that were taken into account were the longitudinal direction along the BM from base to apex and the vertical direction which accounts for the liquid movement perpendicular to the BM. In order to achieve a compact VLSI implementation of the dense resistive network modelling the 2-D cochlea, Van Schaik used a single transistor implementation of the resistors. That transistor was operating in the pseudo-voltage domain and its resulting pseudo-conductance has been proven efficient in a variety of signal processing systems (Vittoz, 1997). To introduce temporal processing, the pseudo-conductance was used with a reactive component (a pseudo-transcapacitor where its differential input current is integrated into an output pseudo-voltage) yielding filters which are close relatives to log-domain filters.
2002 – 2004: From 2002 onwards ***Sarpeshkar's*** auditory research interest seemed to focus on fully-implantable CIs based on simple BP filterbanks. Together with his group at MIT, he published several conference and journal articles detailing the designs of the basic building blocks comprising a CI processor. He reported on the designs of a new BP filter (Salthouse and Sarpeshkar, 2003), envelope detector (Zhak et al., 2003), microphone preamplifier (Baker and Sarpeshkar, 2003) and A/D converter (Sit and Sarpeshkar, 2004) that were consequently used to realise a CI channel (Lu et al., 2003) and a CI processor (Baker et al., 2003). In 2005, all these designs were integrated to create one of the most complete analogue VLSI CIs to date. Sarpeshkar approach in this work was slightly different from what he had adopted in his earlier attempts. Here, he tried to create circuits that would eventually lead to a practical bio-inspired design having the potential towards possible commercialization. For this reason, his architectural and circuit design choices did not solely rely on increasing the performance but also on reliability and robustness. An example of this strategy can be seen in the design of his new BP filters. Sarpeshkar realized that while the linearization techniques used in his prior designs (from 1996 to 1998) successfully met the design requirements, the linear range could not be easily increased above the achieved value because the techniques do not scale. Recall that much of the achieved increase in linear range was due to the well as the input terminal. That makes the linear range a strong function of the subthreshold body-effect parameter n which varies between processes and runs. Hence, Sarpeshkar tried to explore alternative strategies.
The BP filters used in this work were based on the design of ***Christopher Salthouse*** who used a capacitive-attenuation technique to extend the input linear range beyond $1V_{pp}$ (Salthouse and Sarpeshkar, 2003). His design was based on two cascaded first-order sections; one LP and one HP built using the basic OTA. The linear range was increased by attenuating the input and feedback attenuating the output because the linear range of the OTAs is limited by their input swing rather than their output swing. Salthouse consequently extended his design to a differential topology and measured a cascade of two BP filters. He reported a 230nW power consumption with an input DR of 67.5dB (5% THD) at 100Hz – 200Hz range and a 6.36μW with a DR of 65dB (5% THD) at 5kHz – 10kHz range.
In 2002, ***David Graham*** with ***Paul Hasler*** from Georgia Tech presented a new very compact second-order section for cochlea modelling with high overall performance (Graham and

Hasler, 2002). Their design was based on the DIFF2 structure discussed by Lyon in 1992 and on the autozeroing second-order section presented by the authors in (Hasler et al.,). The basic building block of their design is a capacitively-coupled current-conveyor (C^4) presented in (Hasler et al., 1999). In this paper, they presented only measured frequency response results from a 32-section C^4 BP filterbank, whereas a thorough analysis and characterization of the C^4 structure was presented five years later (Graham et al., 2007). There, they demonstrated an impressive five-orders of magnitude frequency tunability with passband SNR generally ranging between 50 – 60dB. At 20kHz and with a Q of 4, the second-order C^4 BP section dissipated a mere 0.11μW of static power from a 3.3V power supply and with a Q-programmability range of up to 9. The simple second-order section occupied 2100μm² in a 0.5μm CMOS process, whereas a tenth-order structure occupied an area of 13200μm². Because of the fact the C^4 was so compact, a filterbank employing sixteen tenth-order BP filters occupied only 1.5mm×1.5mm including all biasing circuits. Finally, the authors were the first to use floating-gate transistors for the current-sources that set the time constants of the C^4 BP filters. Since the floating-gate transistor currents can be programmed very precisely (< ±0.2% error), the responses of the BP filters were also set very precisely using a single calibration step.

In 2003, ***Øivid Næss***, a student of Tor Sverre Lande from the University of Oslo, presented a low-voltage, low-power second-order filter consisting of six pseudo floating-gate transistors operating in the WI (Naess et al., 2003). Næss recalled that in 1998 Sarpeshkar used offset adaptation circuitry in between each stage to limit the skew in offset/DC voltages through his BM cascade. By employing the pseudo floating-gate technique, such offset adaptation circuitry would not be necessary due to the capacitive coupling of the floating-gate nodes. The term 'pseudo' arises from the fact that the floating nodes are not truly floating but weakly connected. Nonetheless, the quiescent currents are still very low giving pseudo floating-gates the same advantage. Additional benefits of this technique include the possibility of operating them with very low-power, shifting the devices' threshold voltages as seen from their capacitive coupled input terminals and an easy initialization/programmability of their floating-gate voltages. Finally, Næss provided preliminary frequency response simulation results from a cascade of six biquads and reported a 5nW power dissipation with a –60dB suppression of the second harmonic at 1kHz from a single second-order LP stage.

The two last contributions came from ***Ivan Grech*** from the University of Surrey who published two journals with detailed measurements on a new low-power log-domain CMOS filterbank for extracting localization spectral cues from two audio signals (Grech et al., 2003; Grech et al., 2004). As far as we are aware, Grech's implementation is the first log-domain realization of a front-end for 2-D sound source localization. Moreover, it is the first ever effort which employed high-performance log-domain biquads operating in Class-AB. All additional circuits were current-mode translinear loops used for performing mathematical operations like squaring, division and maximum value detection. The inputs to the system, which were left and right ear audio signals were converted to current signals and then splitted into complementary differential signals using the harmonic mean splitting law. These signals were then logarithmically compressed after having their level adjusted by a current-mode, open-loop AGC block which acted globally altering the Q values of the subsequent BP filters. Each path was then processed by a parallel bank of 24 fourth-order BP log-domain filters whose CF changed from 50Hz to 20kHz in an exponentially decreasing fashion. Envelop processing was realized at the outputs of each BP filter by squaring and LP

filtering. Envelopes for CFs below 1kHz were further processed off-chip to extract interaural phase delay (IPD)[2] cues, whereas higher frequency envelopes were used to extract interaural envelope delays (IED)[3] cues. Finally, interaural intensity difference (IID)[4] cues were extracted by dividing the envelopes of the left- and right-channels, whereas monaural[5] cues were extracted by dividing the envelopes of adjacent filters of the same channel. Grech's design has one of the highest performances reported to date with a measured BP stage input DR of 62dB at 1.8% THD (in excess of 80dB for the 4–5% THD figures used by other authors), second-order intermodulation distortion products below –40dB and an overall power dissipation of 890μW for the whole system. Moreover, he used on-chip, temperature independent biasing and a *Q*-value digital calibration memory for manually resetting a uniform peak response to all the BP stages. It should be noted that the maximum *Q* reported was 10.25 resulting in a measured passband gain of around 40dB.

2005 & 2006: Five years after Germanovix' CI effort, ***Julio Georgiou***, his successor in Toumazou's group at Imperial College London, was actually the first to validate a 16-channel fully-implantable log-domain CI prosthesis system (Georgiou and Toumazou, 2005a). Georgiou's system occupied an area of 3.4mm×6mm and consisted of a) a mixed-signal chip that combined the speech processor (utilizing a 16-channel Class-A BP log-domain filterbank) and CIS stimulator, b) a rechargeable battery and c) a second chip for power management and charging circuits. The whole system was encapsulated in a hermetically sealed platinum case for biocompatibility reasons. Georgiou reported on a total of 126μW power consumption (including an off-chip microphone but excluding the CIS stimulation) and an input DR (at the BP pole frequencies) between 51 – 58dB for a 4% THD. His filters were Class-A log-domain filters with a state-elimination circuitry (to eliminate additional existing DC operating points (Fox and Nagarajan, 1999)) and a nominal power dissipation of only 40nW. It should be noted here that Georgiou performed rectification, compression and smoothing elegantly and with minimal power requirements by using a circuit that was identical to the nonlinear LP filtering stage used by Van Schaik in his IHC circuit model. Finally, Georgiou employed a digital AGC, in the form of saturation nonlinearity that acted globally on the input prior to being fed to the filterbank. In addition, it was also possible to externally program its attack and release time constants so that it responded more quickly to increasing amplitudes than to decreasing ones. On the other hand, ***Sarpeshkar's*** final CI was also reported in 2005 (Sarpeshkar et al. 2005). Their design achieved a total power consumption of 211μW (including microphone and stimulation circuits), a DR of 77dB and occupied an area of 9.58mm×9.23mm. The basic circuit building blocks comprising their design were:

1. A build-in microphone front-end (using the commercial JFET-buffered FG3329) electret microphone to transduce sound into an electrical signal. The microphone front-end was designed to have an 80dB input DR and its total power consumption was at 100μW (almost half the power dissipation of the whole CI).

[2] IPD represents the time delay between the left and right channels for actual input signals of frequencies below 1kHz.

[3] IED is the same as IPD only for higher frequencies.

[4] IID represent the difference in signal intensity between the left and right channels.

[5] Monaural cues are directly related to intensity differences between adjacent frequency bands of the same channel.

2. An AGC circuit that was implemented by regulating the transconductance of a single transconductance-resistance variable gain amplifier (VGA). The signal from the microphone front-end was passed through an envelope detector (a cascade of a rectifier and LP filter) and consequently fed to a translinear circuit used to create the compressed output current for controlling the gain of the VGA. Moreover, the envelope detector had an asymmetry in its attack and release time constants. Their AGC had an effective 60dB of DR and a power consumption of 30μW.
3. A 16-channel filterbank employing Salthouse's fourth-order BP filters.
4. A logarithmic A/D with 7-bit precision at 1kHz sampling rate with 3μW/channel.
5. High PSRR and temperature independent current and voltage biasing with a total power dissipation of 3μW.
6. Digital I/O interface and CIS stimulator dissipating 32μW.

The last 2005 contribution came from ***Christopher Galbraith*** who reported on a planar channelizer filter (i.e. a microwave multiplexer with a large number of output ports) based on a model of the mammalian cochlea operating at 20–90MHz. Applications of such a bio-inspired system could include wideband electronic warfare systems and radio astronomy and spectroscopy. The channelizer filter topology was derived from the transmission-line model of the cochlea and he reported measured results from a 20-channel prototype chip (Galbrdith et al., 2005;Galbraith et al., 2007). The second RF cochlea followed one year later from ***Sarpeshkar*** (Mandal et al., 2006).

Finally, one of the most recent neuromorphic efforts came from ***Bo Wen*** and ***Kwabena Boahen*** from Stanford University, where they presented a 2-D nonlinear cochlea model utilizing a novel active mechanism that realizes the frequency-selective OHC-based AGC (Wen and Boahen, 2006). Their AGC is based on a model of OHC electromotility through active bi-directional coupling that was initially proposed by Geisler and Sang in 1995 (Geisler and Sang, 1995) and later extended by the authors in (Wen and Boahen, 2003). Their hypothetical model includes *both feed-forward and feed-backward interactions* supported by the physiological evidence:

1. The force resulting from OHC contraction and elongation is exerted onto adjacent downstream BM segment due to the OHC basal tilt.
2. The OHC force is delivered onto adjacent upstream BM segment due to the apical tilt of the phalangeal process extending from the Deiter's cells' main trunk.

Thus, the OHC motile forces, through the microanatomy of the cochlea partition, feed forward and backward, in harmony with each other, resulting in bi-directional coupling between adjacent stages in the longitudinal direction. More specifically, due to the opposing action of the OHC forces on the BM and reticular lamina, the $i^{th} - 1$ BM segment reinforces that of segment i, while the motion of segment $i^{th} + 1$ opposes that of segment i.

Their cochlea processor was built along the same lines with Watts' and Van Schaik's 2-D implementations. Wen's fluid network was implemented by an array of diffusors (i.e. simple NMOS transistors in WI), while each BM segment was realized using pseudo-differential Class-AB log-domain filters. The active bi-directional coupling was achieved by exchanging currents between neighbouring second-order sections, thus realizing an AGC mechanism without needing to detect the signal amplitude and implement AGC loops. Wen reported results from a fabricated chip with 360 BM segments and two 4680-element fluid grids (360×13) occupying 10.9mm^2 area in a 0.25μm CMOS technology. However, Wen's frequency responses seemed to be heavily affected by noise and mismatch resulting in quite

low DR performances (17 – 42dB), which generally are not indicative of pseudo-differential Class-AB log-domain implementations.

2007: In this year, most contriburions came from ***Van Schaik's*** group at the University of Sydney. The first one was a conference publication where his student ***Tara Julia Hamilton*** presented a BM resonator segment together with a feed-backward AGC control loop for 2-D cochlea implementations (Hamilton et al., 2007). The resonator stage was a Class-A log-domain filter whereas the feedback AGC loop was comprised of a peak detector, a decision circuit, a ramp generator and Sarpeshkar's WLR. The output signal level from the BM resonator was measured using the peak detector (again a variation of the nonlinear LP filter Van Schaik and Georgiou used in (Schaik, 2001) and (Georgiou and Toumazou, 2005b), respectively) and then fed into the decision circuit. The decision circuit was consisted of two current comparators with some additional digital logic for setting the ceiling and thresholds of the signal amplitudes (i.e. essentially specifying the Q-control law). In addition, the decision circuit employed hysteresis to avoid errors due to oscillations. The Q value of the resonator stage was set by the WLR's output current whose value was controlled by the voltage from the ramp generator. A higher voltage generated a larger current and thus a larger Q value. When the ramp generator's output voltage was equal to the supply voltage, the WLR's output current was set to give the maximum Q value. Finally they reported preliminary simulated results on a) the manual Q adaptation of the BP log-domain frequency response, b) transient responses from the outputs of each AGC processing stages and c) the actual nonlinear input-output compressive function of their AGC.

The final contributions came from ***Vincent Chan***, ***Shih-Chii Liu*** and Van Schaik who presented a matched silicon cochlea pair with address event representation (AER) designed for sound localization applications (Vincent et al., 2007). In recent years, the AER interface has become the standard interface protocol for a plethora of neuromorphic (mostly vision) chips because it allows the use of discrete level (spikes), continuous-time events to convey information in a manner similar to the pulse code neural communication and processing schemes found in biological systems. The AER allows multiple devices to share a common data bus by using a hand-shaking protocol that arbitrates between transmitters to determine which transmitter can access the bus. The next transmission is not permitted unless an acknowledgment is returned from the receiver. This event-driven representation is ideal for communicating sparse events from many sources using a narrow channel, utilizing effectively the available power and bandwidth.

One of the prior cochlea designs that utilized such a scheme is (Abdalla and Horiuchi, 2005). Their system was comprised of four main building blocks: a) two matched, 32-section, constant-Q and passive (Q = 0.75) silicon cochleae (identical to the one presented in [ ]), b) a new simplified version of Van Schaik's IHC circuit (due to the other's increased complexity and size), c) integrate-and-fire neurons for the AER and d) the AER interface circuitry to generate and communicate auditory nerve spikes. Thus, the output at each BM tap gets half-wave rectified and LP filtered (effect of IHC), and consequently integrated on the membrane capacitance of the integrate-and-fire neuron which fired a spike. The neuron's operation is similar to the one presented in (Schaik, 2001) with two additional voltage lines: the request (req) and acknowledgement (ack) which set and reset it, respectively: When a spike is generated, the req line goes low. A high pulse in the ack line resets the neuron, after which it enters a refractory period for a controllable duration. When a neuron makes a request (by pulling its req signal low), an on-chip arbiter arbitrates between all neurons making a request and sending off each neuron's address in sequence through two external hand-

shaking signals. Once the neuron's address has been communicated off-chip, the arbiter sends a signal to the ack line which in turns resets the neurons.
The authors provided an analysis on the mismatch, offset and gain errors of their system with additional measured results on a sound localization experiment performed in a reverberant realistic environment. They placed a dummy head at the centre of a room facing a loudspeaker with two microphones inserted in its ears. The recorded sounds were played to the left and right cochleae through a soundcard. The dummy head was rotated from –90^{o} to +90^{o} in 5^{o} steps and interaural time delay (ITD) cues were extracted by performing cross-correlation on the spike trains between all corresponding channels. Fig. 31 shows that the calculated delay had a sinusoidal shape with the maximum delays occurring close to the two 90^{o} angle extremes as expected.

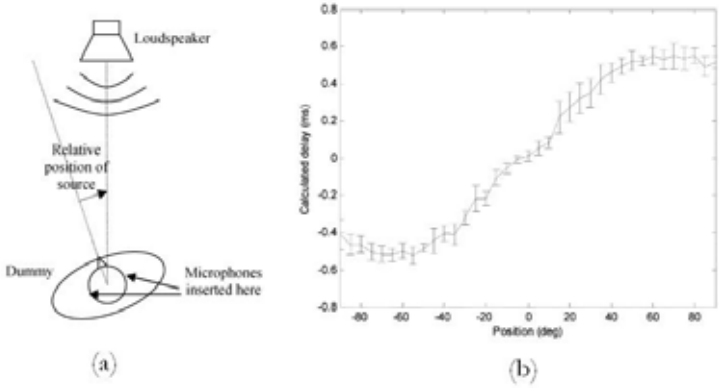

Fig. 31. (a) Experimental setup. The source was fixed but the dummy is free to rotate from –90^{o} to +90^{o} in 5^{o} steps. Microphones were inserted into its ear to record the sound at each position. (b) ITD computed by cross-correlation of the spike trains from all channels of the two matched silicon cochleae; adapted from Chan (Vincent et al., 2007).

2009: Our final contribution is from ***Andreas Katsiamis***, who designed a very-high dynamic range and low-power cochlea channel with focus on biorealism and performance (Katsiamis A.G. et al. 2009). The design implements a recently proposed transfer function, namely the One-Zero Gammatone Filter (or OZGF), which provides a robust foundation for modeling a variety of auditory data such as realistic passband asymmetry, linear low-frequency tail and level-dependent gain (Katsiamis A.G. et al., 2007). Moreover, the OZGF is attractive because it can be implemented efficiently in any technological medium – analogue or digital – using standard building blocks. The channel was synthesized using novel, low-power, Class-AB, log-domain, biquadratic filters employing MOS transistors operating in their weak inversion regime. In addition, his work details the design of a new low-power automatic gain control circuit that adapts the gain of the channel according to the input signal strength, thereby extending significantly its input dynamic range. The performance of a 4th-order OZGF channel (equivalent to an 8th-order cascaded filter structure) was evaluated through both detailed simulations and measurements from a fabricated chip using the commercially available 0.35μm AMS CMOS process. The whole system was tuned at 3kHz, dissipated a mere 4.46μW of static power, accommodated 124dB (at <5% THD) of input dynamic range at the center frequency and was set to provide up to 70dB of amplification for small signals.

4. Summary and conclusion

This chapter has hopefully served two main purposes: a) to form a detailed review of all the important developments on the modelling, design and experimental verification of CMOS VLSI cochlea processors, and b) to equip the reader with the general knowledge needed so that s/he can appreciate the design/modelling efforts presented in the following chapters.
This chapter discussed in considerable detail most of the advancements on the modelling and design of CMOS VLSI cochlea systems from 1982 until recently. From Lyon's initial 1982 and 1988 papers, there were numerous attempts from various research groups to extend and optimize the design of cochlea processors for applications including cue extraction for source localization, cochlea implants and general speech recognition front-ends. In this chapter we reviewed the application of voltage mode (g_m-C), discrete-time (switch-capacitor and switch-current), current-mode (switch-current, log-domain and current-conveyor-based) and even microwave-RF circuit design techniques in pursue of cochlea processors of an increased overall performance. We also saw several variations in the architecture of the BM filtering (1- and 2-D BM cascade, simple BP filterbanks, parallel banks of cascaded filters, dilating-biquads filterbanks and variable clock-frequency filterbanks) and bio-plausible designs of IHC and neuron circuits together with several versions of the OHC-based AGC (static compression, feedback, feed-forward or both). In conclusion, the design of artificial cochlea systems able to exhibit a high overall performance with a high degree of biological fidelity was and very much still is a perpetual objective.

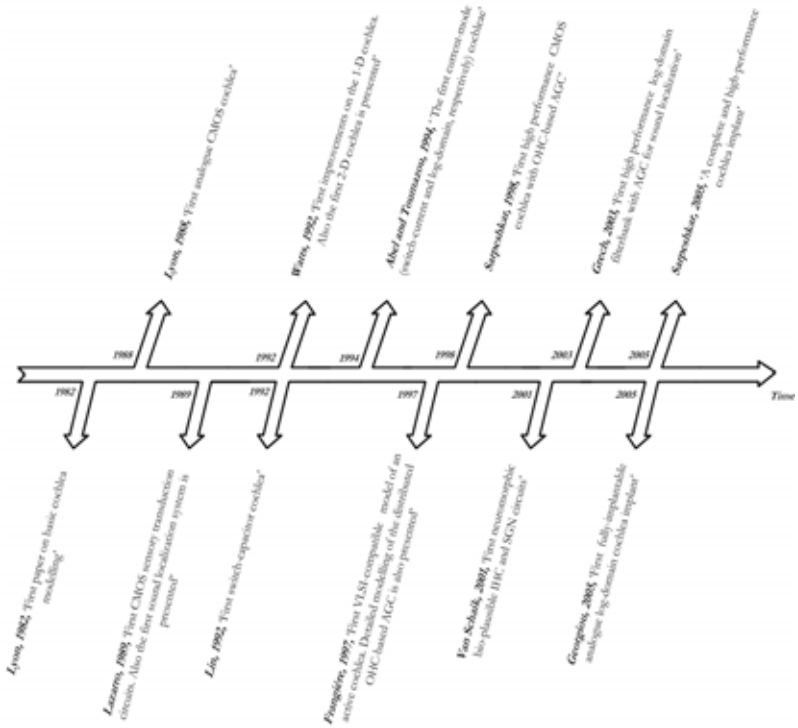

Fig. 32. Timeline of most important CMOS Cochlea Advancements.

Table 1. Summary of Developments of Analogue VLSI Cochlea Systems

Authors	Description – Application	IHC/OHC/SGN	Architecture	Stages/ Channels	Method	Power	DR	Size
R.F. Lyon	1st CMOS Cochlea	No	Filter-Cascade	480	g_m-C	N/A	N/A	N/A
J. Lazzaro	1st Sound Localization System	Yes	Filter-Cascade	62x2	g_m-C	N/A	60dB	N/A
L. Watts	1st Improved 1-D Cochlea	No	Filter-Cascade	43-51	g_m-C	11µW	N/A	5mm²
W. Liu	Speech Recognition	Yes/Yes/No	Filter-Cascade	30	g_m-C	15µW	50dB	4.84mm²
J. Lin	Cochlea Filters	No	FilterBank	32	Switch-Cap	N/A	N/A	N/A
N. Bhadkamkar	Sound Localization	Yes	Filter-Cascade	60x2	g_m-C	N/A	N/A	N/A
L. Watts	1st 2-D Cochlea	No	Resistive Grid	61x5	g_m-C	N/A	N/A	31.28mm²
N. Bhadkamkar	Sound Localization	Yes	FilterBank	25x2	g_m-C	N/A	N/A	31.28mm²
J. Lin	Auditory Wavelet Transform	No	FilterBank	32	Switch-Cap	N/A	N/A	31.28mm²
C. Toumazou	Cochlea Filters	No	N/A	1	Log-domain	0.25µW	80dB	N/A
C. Abel	CMOS Cochlea	No	Filter-Cascade	16	Switch-Current	N/A	N/A	N/A
Y.C. Chen	Circuits for Cochlea Implants	Yes/No/Yes	Filter-Cascade	30	g_m-C	N/A	N/A	N/A
P. Furth	Architectural Investigation	No	Filter-Bank	16	g_m-C	355nW	28dB	N/A
P. Furth	OTA Designs	No	N/A	N/A	g_m-C	N/A	48-51dB	N/A
J.C. Bor	SC Cochlea Processor	No	Filter-Cascade	32	Switch-Cap	N/A	67dB	12.25mm²
R. Sarpeshkar	1st Active Cochlea	No/Yes/No	Filter-Cascade	45	g_m-C	N/A	60dB	4.84mm²
A. Van Schaik	2nd Improved 1-D Cochlea	No	Filter-Cascade	104	g_m-C	N/A	N/A	15.3mm²
P. Furth	OTA Designs	No	N/A	N/A	g_m-C	N/A	66dB	N/A
E. Fragniére	Active Cochlea Model	Yes/Yes/No	Filter-Cascade	N/A	g_m-C	N/A	N/A	N/A
R. Sarpeshkar	1st Active Cochlea Chip	Yes/Yes/No	Filter-Cascade	117	g_m-C	0.5mW	61dB	7.7mm²
R. T. Edwards	Cochlea BP Filterbank	No	N/A	15	Log-domain	N/A	N/A	N/A
N. Kumar	Speech Recognition	No	Filter-Cascade	15	Mixed-Signal	N/A	N/A	4mm²
T. Hinck	Current-mode Cochlea	No	TWamp	100	Current-mode	N/A	54dB	N/A
R. T. Edwards	Auditory Log-domain Circuits	No	Filter-Bank	15	Log-domain	200µW	35dB	4mm²
W. Germanovix	1st Analogue CI	No	Single-Channel	1	Log-domain	N/A	N/A	N/A
A. Van Schaik	Periodicity Extraction	Yes/Yes/Yes	Filter-Cascade	104	g_m-C	>25mW	N/A	15.3mm²
A. Van Schaik	A 2-D CMOS Cochlea	No	Resistive Grid	100	P-V domain	N/A	N/A	N/A
D. Graham	10th-order BP Filters	No	Filter-Bank	16	Current-Conveyor	0.11µW/ stage	N/A	2.25mm²
C. Salthouse	4th-order BP Filter for CI	N/A	N/A	1	g_m-C	6.36µW	65dB	N/A
ØNœss	LP biquad for CMOS Cochlea	N/A	N/A	1	Floating-Gate	4.8nW	N/A	N/A
M. W. Baker	Analogue FilterBank for CI	No	Filter-Bank	16	g_m-C	470µW	51dB	88.4mm²
I. Grech	2-D Sound Localization	Yes/Yes/No	Filter-Bank	24x2	Log-domain	890µW	>>62dB	143mm²
J. Georgiou	1st Fully-Implantable CI	Yes/Yes/No	Filter-Bank	16 (2x8)	Log-domain	126µW	51-58dB	21mm²
R. Sarpeshkar	A High-Performance CI	Yes/Yes/No	Filter-Bank	16	g_m-C	211µW	77dB	88.4mm²
B. Wen	2-D Active Cochlea	Yes/Yes/No	Resistive Grid	360	Log-domain	52mW	17-42dB	10.9mm²
V. Chan	2-D Cochlea with AER	Yes/No/Yes	Filter-Cascade	32x2	g_m-C	N/A	N/A	5.4mm²
A. Katsiamis	OZGF Channel with AGC	Yes/Yes/No	Filter-Cascade	4x1	Log-domain	4.46µW	124dB	2.25mm²

One may be caught by surprise to realize the fact that the engineering principles the real cochlea is using are not conceptually far from what we had developed over the years to solve various engineering problems: Master/Slave architectures with automatic control for tuning and stabilization, compression for the accommodation of large inputs, gain adaptation to maintain signal integrity, rectification and filtering for strength detection, parallel processing (i.e. redundancy) to increase speed and robustness, to name just a few, are concepts that were developed by engineers who might had not 'made the link' with biological correlates. Yet, nature had all these ideas for millions of years and had already optimized them to realise systems which are able to perform with astonishing reliability in the haziest of environments. The cochlea is just one of those systems and to this author's opinion this is exactly the scientific contribution of neuromorphic engineering.

5. Reference

A.Van Schaik, E.Fragniere, E.Vittoz. 1996. Improved Silicon Cochlea using Compatible Lateral Bipolar Transistors, In: D.Touretzky et al., editor. *Advances in Neural Information Processing Systems 8*. Cambridge MA: MIT press. p 671-677.

Abdalla H, Horiuchi TK. 2005. An ultrasonic filterbank with spiking neurons. Circuits and Systems, 2005 ISCAS 2005 IEEE International Symposium on4201-4204.

Abel C, Park J, Ismail M, Lohiser B, Justice S, Bibyk S, Fiez T. 1994. A switched-current silicon cochlea. Neural Networks, 1994 IEEE World Congress on Computational Intelligence , 1994 IEEE International Conference on 3.

Andreou AG, Liu W. BiCMOS circuits for silicon cochleas. European Conference on Circuit Theory and Design503-508.

Baker MW, Lu TKT, Salthouse CD, Sit JJ, Zhak S, Sarpeshkar R. 2003. A 16-channel analog VLSI processor for bionic ears and speech-recognition front ends. Custom Integrated Circuits Conference, 2003 Proceedings of the IEEE 2003521-526.

Baker MW, Sarpeshkar R. 2003. A low-power high-PSRR current-mode microphone preamplifier. Solid-State Circuits, IEEE Journal of 38:1671-1678.

Bhadkamkar N. 1993. A Variable Resolution, Nonlinear Silicon Cochlea. Computer Systems Laboratory, Stanford University.

Bhadkamkar N, Fowler B. 1993. A sound localization system based on biological analogy. Neural Networks, 1993 , IEEE International Conference on1902-1907.

Bhadkamkar NA. 1994. Binaural source localizer chip using subthreshold analog CMOS. Neural Networks, 1994 IEEE World Congress on Computational Intelligence , 1994 IEEE International Conference on 3:1866-1870.

Boahen KA, Andreou AG. 1992. A contrast sensitive silicon retina with reciprocal synapses. Advances in Neural Information Processing Systems 4:764-772.

Bor JC, Wu CY. 1996. Analog electronic cochlea design using multiplexing switched-capacitor circuits. Neural Networks, IEEE Transactions on 7:155-166.

Chang JS, Tong YC. 1990. A pole sharing technique for linear phase switched-capacitor filterbanks. Circuits and Systems, IEEE Transactions on 37:1465-1479.

Chen YC, Chen JH. 1994. An analog CMOS circuit for cochlea implant. Engineering in Medicine and Biology Society, 1994 Engineering Advances: New Opportunities for Biomedical Engineers Proceedings of the 16th Annual International Conference of the IEEE978-979.

Delbruck T. 1991. Bump circuits for computing similarity and dissimilarity of analog voltages. Neural Networks, 1991 , IJCNN-91-Seattle International Joint Conference on 1.

Edwards RT, Cauwenberghs G. A second-order log-domain bandpass filter for audio frequency applications. Circuits and Systems, 1998.ISCAS '98.Proceedings of the 1998 IEEE International Symposium on 3, p 651-654. 1998.

Ref Type: Internet Communication

Edwards RT, Cauwenberghs G. 1999. Log-domain circuits for auditory signal processing. Circuits and Systems, 1999 42nd Midwest Symposium on 2.

Fletcher H. 1930. A SPACE-TIME PATTERN THEORY OF HEARING. The Journal of the Acoustical Society of America 1:311-343.

Fox RM, Nagarajan M. 1999. Multiple operating points in a CMOS log-domain filter. Circuits and Systems II: Analog and Digital Signal Processing, IEEE Transactions on 46:705-710.

Fragniere E. 1998. Analogue VLSI Emulation of the Cochlea. PhD thesis, Swiss Federal Institute of Technology (EPFL), Lausanne.

Fragniere E, van Schaik A, Vittoz EA. 1997. Design of an Analogue VLSI Model of an Active Cochlea. Analog Integrated Circuits and Signal Processing 13:19-35.

Frey DR. 1993. Log-domain filtering: an approach to current-mode filtering. Circuits, Devices and Systems, IEE Proceedings G 140:406-416.

Frey DR. 1996. Exponential state space filters: a generic current mode-design strategy. Circuits and Systems I: Fundamental Theory and Applications, IEEE Transactions on 43:34-42.

Furth PM, Andreou AG. 1995a. A design framework for low power analog filter banks. Circuits and Systems I: Fundamental Theory and Applications, IEEE Transactions on 42:966-971.

Furth PM, Andreou AG. 1995b. Linearised differential transconductors in subthreshold CMOS. Electronics Letters 31:545-547.

Furth PM, Andreou AG. 1996a. Cochlear models implemented with linearized transconductors. Circuits and Systems, 1996 ISCAS'96 ,'Connecting the World' , 1996 IEEE International Symposium on 3.

Furth PM, Andreou AG. 1996b. Translinear transconductor design for cochlear filter banks. Circuits and Systems, 1996 , IEEE 39th Midwest symposium on 2.

Galbraith C, Rebeiz GM, Drangmeister R. 2007. A Cochlea-based Preselector for UWB Applications. Radio Frequency Integrated Circuits (RFIC) Symposium, 2007 IEEE219-222.

GALBRDITH C, WHITE R, GROSH K, REBEIZ GM. 2005. A mammalian cochlea-based RF channelizing filter. IEEE MTT-S International Microwave Symposium digest 4:1935-1938.

Geisler CD, Sang C. 1995. A cochlear model using feed-forward outer-hair-cell forces. Hearing Research 86:132-146.

Georgiou J, Toumazou C. 2005a. A 126-/spl mu/W cochlear chip for a totally implantable system. Solid-State Circuits, IEEE Journal of 40:430-443.

Georgiou J, Toumazou C. 2005b. A 126-/spl mu/W cochlear chip for a totally implantable system. Solid-State Circuits, IEEE Journal of 40:430-443.

Germanovix W, Toumazou C. 2000. Design of a micropower current-mode log-domain analog cochlearimplant. Circuits and Systems II: Analog and Digital Signal Processing, IEEE Transactions on 47:1023-1046.

Graham DW, Hasler P. 2002. Capacitively-coupled current conveyer second-order section for continuous-time bandpass filtering and cochlea modeling. Circuits and Systems, 2002 ISCAS 2002 IEEE International Symposium on 5.

Graham DW, Hasler PE, Chawla R, Smith PD. 2007. A Low-Power Programmable Bandpass Filter Section for Higher Order Filter Applications. Circuits and Systems I: Regular Papers, IEEE Transactions on 54:1165-1176.

Grech I, Micallef J, Vladimirova T. 2003. Low-Power Log-Domain CMOS Filter Bank for 2-D Sound Source Localization. Analog Integr Circuits Signal Process 36:99-117.

Grech I, Micallef J, Vladimirova T. 2004. Analog CMOS Chipset for a 2-D Sound Localization System. Analog Integrated Circuits and Signal Processing 41:167-184.

Hamilton TJ, Jin C, van Schaik A. 2007. A Basilar Membrane Resonator for an Active 2-D Cochlea. Circuits and Systems, 2007 ISCAS 2007 IEEE International Symposium on2387-2390.

Hasler P, Kucic M, Minch BA. 1999. A transistor-only circuit model of the autozeroing floating-gate amplifier. Circuits and Systems, 1999 42nd Midwest Symposium on 1.

Hasler P, Stanford T, Minch BA, Diorio C. An autozeroing floating-gate second-order section. Circuits and Systems, 1998 ISCAS'98 Proceedings of the 1998 IEEE International Symposium on 2.

Hinck T, Yang Z, Zhang Q, Hubbard AE. 1999. A current-mode implementation of a traveling wave amplifier modelsimilar to the cochlea. Circuits and Systems, 1999 ISCAS'99 Proceedings of the 1999 IEEE International Symposium on 2.

Hirahara T, Komakine T. 1989. A computational cochlear nonlinear preprocessing model with adaptive Q circuits. Proceedings of IEEE International Conference on Acoustics, Speech and Signal Processing (ICASSP 89) 1:496-499.

Hubbard A. 1993. A traveling-wave amplifier model of the cochlea. Science 259:68-71.

Katsiamis A.G., Drakakis EM, Lyon R.F. A Biomimetic, 4.5 μW, 120+dB, Log-domain Cochlea Channel with AGC. IEEE JOURNAL OF SOLID STATE CIRCUITS 44, p 1006-1022. 2009.

Ref Type: Journal (Full)

Katsiamis A.G., Drakakis EM, Lyon RF. 2007. Practical Gammatone-like Filters for Auditory Processing. EURASIP Journal on Audio, Speech, and Music Processing 2007, 15 Pages.

Kim DO. 1986. Active and nonlinear cochlear biomechanics and the role of outer-hair-cell subsystem in the mammalian auditory system. Hearing Research 22:105-114.

Kim DO, Molnar CE, Pfeiffer RR. 1973. A system of nonlinear differential equations modeling basilar-membrane motion. The Journal of the Acoustical Society of America 54:1517-1529.

Kimura K. 1994. Some circuit design techniques using two cross-coupled, emitter-coupled pairs. Circuits and Systems I: Fundamental Theory and Applications, IEEE Transactions on 41:411-423.

Kimura K. 1995. Circuit design techniques for very low-voltage analog functional blocks using triple-tail cells. Circuits and Systems I: Fundamental Theory and Applications, IEEE Transactions on 42:873-885.

Kumar N, Himmelbauer W, Cauwenberghs G, Andreou AG. 1998. An analog VLSI chip with asynchronous interface for auditoryfeature extraction. Circuits and Systems II: Analog and Digital Signal Processing, IEEE Transactions on 45:600-606.

Lazzaro J. 1991. A silicon model of an auditory neural representation of spectralshape. Solid-State Circuits, IEEE Journal of 26:772-777.

Lazzaro J, Mead C. 1989a. CIRCUIT MODELS OF SENSORY TRANSDUCTION IN THE COCHLEA. Analog VLSI Implementation of Neural Systems.

Lazzaro J, Mead C. 1989b. Silicon Modeling of Pitch Perception. Proceedings of the National Academy of Sciences of the United States of America 86:9597-9601.

Lazzaro J, Mead CA. 1990. A silicon model of auditory localization. Neural Computation 1:47-57.

Lin J, Ki WH, Edwards T, Shamma S, Inc CL, Fremont CA. 1994. Analog VLSI implementations of auditory wavelet transforms using switched-capacitor circuits. Circuits and Systems I: Fundamental Theory and Applications, IEEE Transactions on 41:572-583.

Lin J, Ki WH, Thompson K, Shamma S. 1992a. Cochlear filters design using a parallel dilating-biquadsswitched-capacitor filter bank. Circuits and Systems, 1992 ISCAS'92 Proceedings , 1992 IEEE International Symposium on 4.

Lin J, Ki WH, Thompson K, Shamma S. 1992b. Realization of cochlear filters by VLT switched capacitor biquads. Acoustics, Speech, and Signal Processing, 1992 ICASSP-92 , 1992 IEEE International Conference on 2.

Liu W. 1992. An Analog Cochlear Model Signal Representation and VLSI Realization.

Liu W, Andreou AG, Goldstein MH. 1992. Voiced-speech representation by an analog silicon model of the auditory periphery. Neural Networks, IEEE Transactions on 3:477-487.

Lu TKT, Baker M, Salthouse CD, Sit JJ, Zhak S, Sarpeshkar R. 2003. A micropower analog VLSI processing channel for bionic ears and speech-recognition front ends. Circuits and Systems, 2003 ISCAS'03 Proceedings of the 2003 International Symposium on 5.

Lyon R. 1982. A computational model of filtering, detection, and compression in the cochlea. Acoustics, Speech, and Signal Processing, IEEE International Conference on ICASSP '82 7:1282-1285.

Lyon RF. 1978. A Signal Processing Model of Hearing. found in 'http://www dicklyon com'.

Lyon RF. 1991. Analog Implementations of Auditory Models. DARPA Workshop on Speech Recognition and Natural Language.

Lyon RF, Mead C. 1988a. An analog electronic cochlea. Acoustics, Speech, and Signal Processing [see also IEEE Transactions on Signal Processing], IEEE Transactions on 36:1119-1134.

Lyon RF, Mead CA. 1988b. A CMOS VLSI cochlea. Acoustics, Speech, and Signal Processing, 1988 ICASSP-88 , 1988 International Conference on2172-2175.

Mahowald MA, Delbriick T. 1989. Cooperative Stereo Matching Using Static and Dynamic Image Features. Analog VLSI Implementation of Neural Systems.

Mandal S, Zhak S, Sarpeshkar R. 2006. Circuits for an RF Cochlea. Circuits and Systems, 2006 ISCAS 2006 Proceedings 2006 IEEE International Symposium on4.

Mead C. 1989. Analog VLSI and neural systems. Addison-Wesley Longman Publishing Co., Inc. Boston, MA, USA.

Mead C. 1990. Neuromorphic electronic systems. Proceedings of the IEEE 78:1629-1636.

Naess O, Olsen EA, Berg Y, Lande TS. 2003. A low voltage second order biquad using pseudo floating-gate transistors. Circuits and Systems, 2003 ISCAS'03 Proceedings of the 2003 International Symposium on 1.

Namasivayan AK. 2004. Cochlear Implant Technical Issues: Electrodes, Channels, Stimulation Modes and More. AudiologyOnline, Archives.

Salthouse CD, Sarpeshkar R. 2003. A practical micropower programmable bandpass filter for use in bionic ears. Solid-State Circuits, IEEE Journal of 38:63-70.

Sarpeshkar R, Lyon R.F., Mead C. 1998. A Low-Power Wide-Dynamic-Range Analog VLSI Cochlea. Analog Integrated Circuits and Signal Processing 16:245-274.

Sarpeshkar R, Lyon RF, Mead CA. 1996. An analog VLSI cochlea with new transconductance amplifiers and nonlinear gain control. Circuits and Systems, 1996 ISCAS '96 , 'Connecting the World' , 1996 IEEE International Symposium on 3:292-296.

Sarpeshkar R, Salthouse C, Ji-Jon S, Baker MW, Zhak SM, Lu TKT, Turicchia L, Balster S. 2005. An ultra-low-power programmable analog bionic ear processor. Biomedical Engineering, IEEE Transactions on 52:711-727.

Schaik A. 2001. An Analog VLSI Model of Periodicity Extraction in the Human Auditory System. Analog Integrated Circuits and Signal Processing 26:157-177.

Seevinck E. 1990. Companding current-mode integrator: A new circuit principle for continuous-time monolithic filters. Electronics Letters 26:2046.

Sit JJ, Sarpeshkar R. 2004. A micropower logarithmic A/D with offset and temperature compensation. Solid-State Circuits, IEEE Journal of 39:308-319.

Slaney M. 1988. Lyon's Cochlear Model. Apple Computer, Advanced Technology Group.

Smith RL, Brachman ML. 1982. Adaptation in auditory-nerve fibers: A revised model. Biological Cybernetics 44:107-120.

Toumazou C, Ngarmnil J, Lande TS. 1994. Micropower log-domain filter for electronic cochlea. Electronics Letters 30:1839-1841.

Tsividis YP, Gopinathan V, Toth L. 1990. Companding in signal processing. Electronics Letters 26:1331-1332.

van Schaik A. 2003. A small analog VLSI inner hair cell model. Circuits and Systems, 2003 ISCAS'03 Proceedings of the 2003 International Symposium on 1.

Van Schaik A, Fragniere E. 2001. Pseudo-voltage domain implementation of a 2-dimensional silicon cochlea. Circuits and Systems, 2001 ISCAS 2001 The 2001 IEEE International Symposium on 3.

van Schaik A, Meddis R. 1996. The electronic ear; towards a blueprint. Neurobiology233-250.

Vincent C, Shih-Chii L, Andre VS. 2007. AER EAR: A Matched Silicon Cochlea Pair With Address Event Representation Interface. Circuits and Systems I: Regular Papers, IEEE Transactions on 54:48-59.

Vittoz EA. 1983. MOS transistors operated in the lateral bipolar mode and their application in CMOS technology. Solid-State Circuits, IEEE Journal of 18:273-279.

Vittoz EA. 1997. Pseudo-Resistive Networks and their Applications to Analog Collective Computation. Proceedings of the 7th International Conference on Artificial Neural Networks1133-1150.

Watts L. 1992. Cochlear Mechanics: Analysis and Analog VLSI. PhD Thesis, California Institute of Technology.

Watts L, Kerns DA, Lyon RF, Mead CA. 1992. Improved implementation of the silicon cochlea. Solid-State Circuits, IEEE Journal of 27:692-700.

Wegel RL, Lane CE. 1924. The Auditory Masking of One Pure Tone by Another and its Probable Relation to the Dynamics of the Inner Ear. Phys Rev 23:266.

Wen B, Boahen K. 2003. A linear cochlear model with active bi-directional coupling. Engineering in Medicine and Biology Society, 2003 Proceedings of the 25th Annual International Conference of the IEEE 3.

Wen B, Boahen K. 2006. A 360-Channel Speech Preprocessor that Emulates the Cochlear Amplifier. Solid-State Circuits, 2006 IEEE International Conference Digest of Technical Papers2268-2277.

Zhak SM, Baker MW, Sarpeshkar R. 2003. A low-power wide dynamic range envelope detector. Solid-State Circuits, IEEE Journal of 38:1750-1753.

Zwislocki J. 1950. Theory of the Acoustical Action of the Cochlea. The Journal of the Acoustical Society of America 22:778.

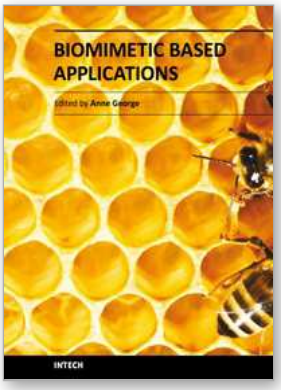

Biomimetic Based Applications

Edited by Prof. Marko Cavrak

ISBN 978-953-307-195-4
Hard cover, 572 pages
Publisher InTech
Published online 26, April, 2011
Published in print edition April, 2011

The interaction between cells, tissues and biomaterial surfaces are the highlights of the book "Biomimetic Based Applications". In this regard the effect of nanostructures and nanotopographies and their effect on the development of a new generation of biomaterials including advanced multifunctional scaffolds for tissue engineering are discussed. The 2 volumes contain articles that cover a wide spectrum of subject matter such as different aspects of the development of scaffolds and coatings with enhanced performance and bioactivity, including investigations of material surface-cell interactions.

How to reference

In order to correctly reference this scholarly work, feel free to copy and paste the following:

Andreas Katsiamis and Emmanuel Drakakis (2011). Analogue CMOS Cochlea Systems: A Historic Retrospective, Biomimetic Based Applications, Prof. Marko Cavrak (Ed.), ISBN: 978-953-307-195-4, InTech, Available from: http://www.intechopen.com/books/biomimetic-based-applications/analogue-cmos-cochlea-systems-a-historic-retrospective

INTECH
open science | open minds

InTech Europe
University Campus STeP Ri
Slavka Krautzeka 83/A
51000 Rijeka, Croatia
Phone: +385 (51) 770 447
Fax: +385 (51) 686 166
www.intechopen.com

InTech China
Unit 405, Office Block, Hotel Equatorial Shanghai
No.65, Yan An Road (West), Shanghai, 200040, China
中国上海市延安西路65号上海国际贵都大饭店办公楼405单元
Phone: +86-21-62489820
Fax: +86-21-62489821